Substantial Contribution of the Two Imidazole Rings of the His13–His14 Dyad to Cu(II) Binding in Amyloid-β (1–16) at Physiological pH and Its Significance

*Byong-kyu Shin and Sunil Saxena**

Department of Chemistry, University of Pittsburgh, 219 Parkman Avenue, Pittsburgh, PA 15260

SUPPORTING INFORMATION

CW-ESR Simulation

The continuous wave electron spin resonance (CW-ESR) spectrum of the nonlabeled Aβ(1−16) peptide mixed with an equimolar amount Cu(II) has two distinguishable components. The simulated spectra of the two components and the best-fit simulated spectra are illustrated in **Figure S1**. The ESR parameters including g values and A values are provided in **Table S1**.

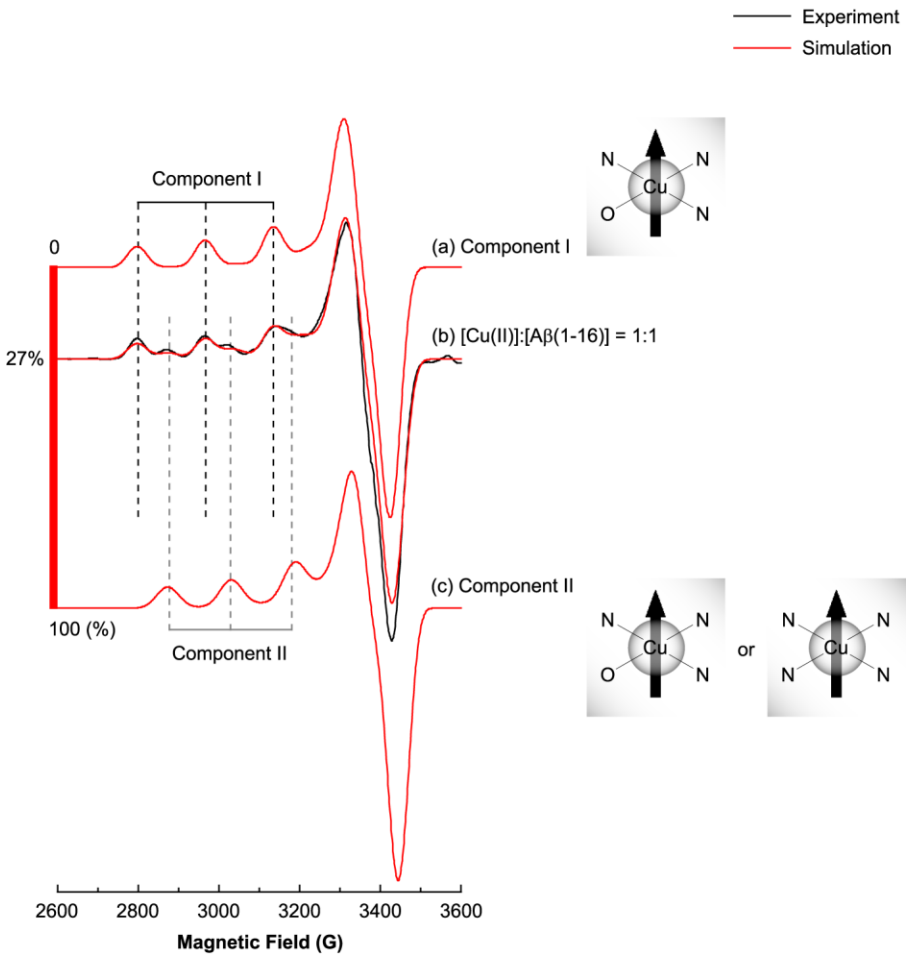

Figure S1. CW-ESR simulation of the nonlabeled Aβ(1−16) peptide mixed with an equimolar amount of Cu(II). The simulated spectra of Component I, Component II, and the mixture thereof are illustrated in red while the experimentally obtained spectrum is in black.

The best-fit simulation is obtained when the contribution of the minor component, Component II, to the spectrum is approximately 27%. Even though the superhyperfine splitting due to three coordinated nitrogen nuclei is considered in Component II, the best -fit spectra are not significantly affected by the

hyperfine constants of nitrogen, $A(^{14}N)$. The simulation results reveal that the two components have a square planar geometry.

Table S1. ESR parameters used for Component I and Component II

	$g_{\|\|}$	$A_{\|\|}$ (G)	$g_{\perp}$	$A_{\perp}$ (G)	$A(^{14}N)$ (G)[a]
Component I	2.27 ± 0.005	171 ± 1	2.06 ± 0.005	15 ± 1	14 ± 1
Component II	2.23 ± 0.005	157 ± 1	2.05 ± 0.005	20 ± 1	15 ± 1

[a] Used for A_{xx}, A_{yy}, and A_{zz} of three Cu(II)-coordinated ^{14}N nuclei

On the other hand, the CW-ESR spectrum of the nonlabeled Aβ(1–16) peptide mixed with an equimolar amount of the Cu(II)–diethylenetriamine (dien) complex has only one component. The best-fit simulated spectrum is illustrated in **Figure S2**. The ESR parameters including g values and A values are provided in **Table S2**.

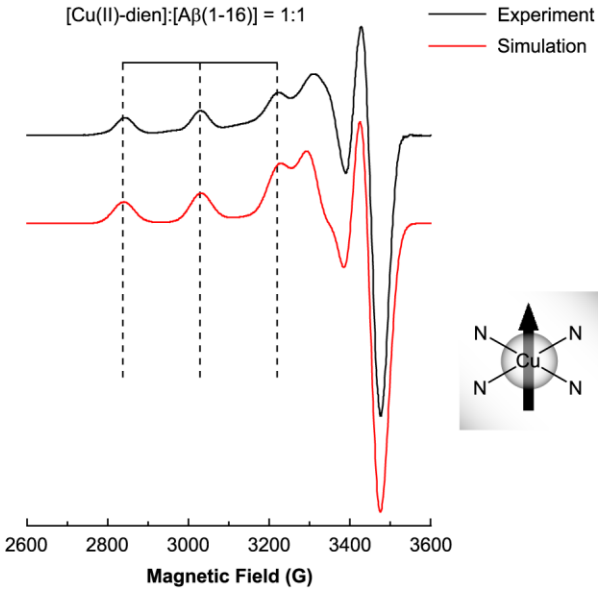

Figure S2. CW-ESR simulation of the nonlabeled Aβ(1–16) peptide mixed with an equimolar amount of the Cu(II)–dien complex. The simulated spectrum is illustrated in red while the experimentally obtained spectrum is in black.

The simulation results reveal that the dien–Cu(II)–Aβ(1–16) complex has a square planar geometry with four nitrogen donors on the plane.

Table S2. ESR parameters used for simulation of the dien–Cu(II)–Aβ(1–16) complex

$g_{\parallel}$	$A_{\parallel}$ (G)	$g_{\perp}$	$A_{\perp}$ (G)
2.21 ± 0.005	191 ± 1	2.05 ± 0.005	30 ± 1

Three-Pulse ESEEM Spectra of the Nonlabeled and ^{15}N-Labeled Cu(II)–Aβ(1–16) Complexes

Three-pulse electron spin-echo envelope modulation (ESEEM) experiments were carried out on the equimolar mixture of Cu(II) and each of Aβ(1–16), Aβ(1–16)H6[^{15}N], Aβ(1–16)H13[^{15}N], and Aβ(1–16)H14[^{15}N] under three different conditions.

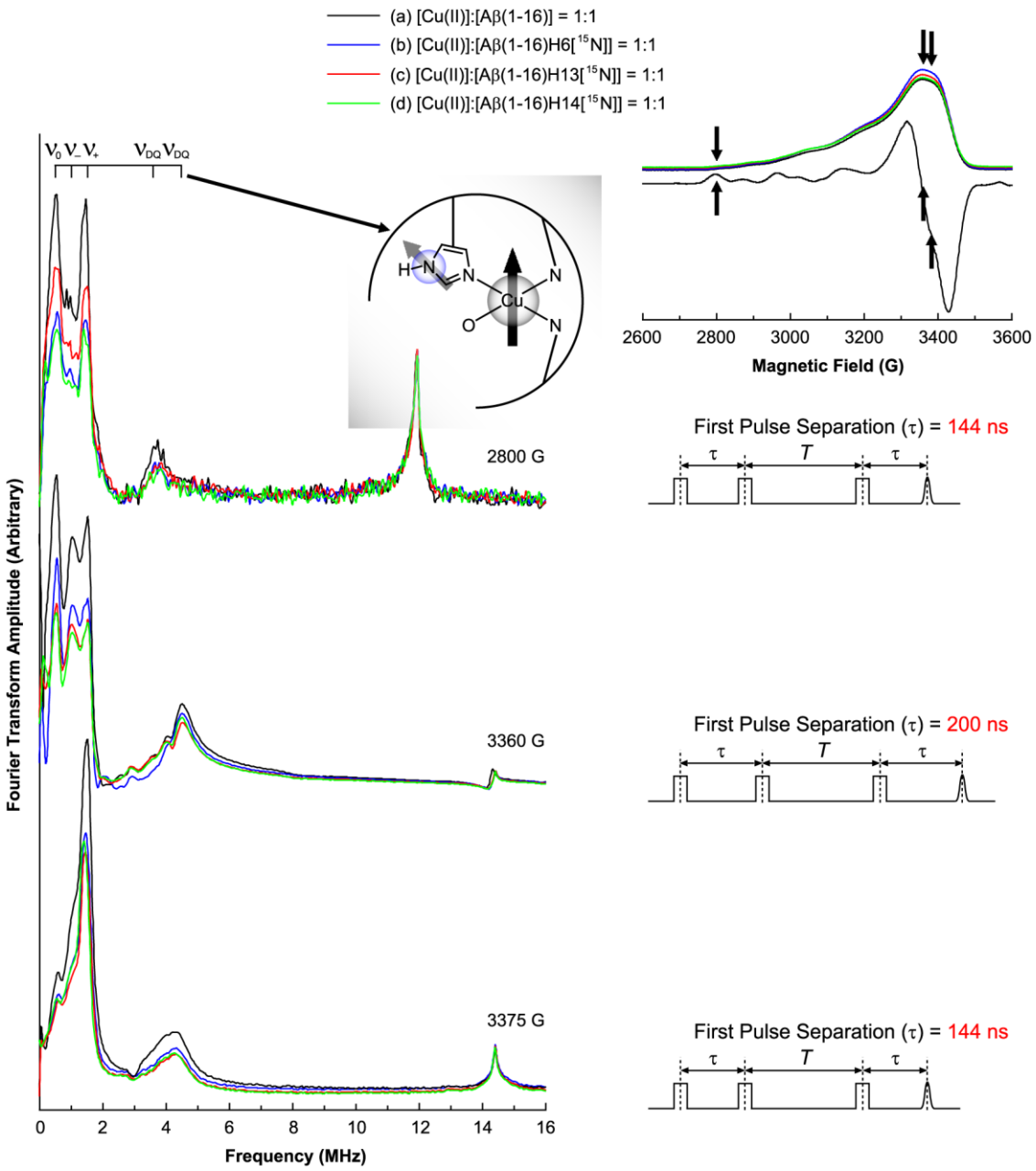

Figure S3. Three-pulse ESEEM spectra of the nonlabeled and ^{15}N-labeled Aβ(1–16) analogues mixed with an equimolar amount of Cu(II) collected under three different conditions. The spectra at the center are obtained at 3360 G with a first pulse separation of 200 ns and an initial second pulse separation of 400 ns and the spectra at the top and at the bottom are at 2800 G and 3375 G, respectively, with a first pulse separation of 144 ns and an initial second pulse separation of 288 ns.

Figure S3 shows the ESEEM spectra obtained at 2800 G, 3360 G, and 3375 G. Each spectrum has peaks at or around 0.55, 1.01, and 1.54 MHz irrespective of the magnetic field and the pulse separations. Regarding the three peaks at or around 0.55, 1.01, and 1.54 MHz, the sum of the lower two frequencies equals the highest one, which indicates the peaks are mainly due to the three different transitions between nuclear quadrupole levels of a ^{14}N nucleus. On the other hand, a broad peak appears around 4.4 MHz in the spectra obtained at 3360 G and 3375 G while the broad peak shifts to around 3.8 MHz in the spectra obtained at 2800 G. The dependence of the frequency on the magnetic field, along with the peak position, strongly suggests that the peaks appearing around 3.8 MHz or 4.4 MHz are due to the double-quantum (DQ) transition of a ^{14}N nuclear spin in the other electron spin manifold.

Time-Domain Curves of the Nonlabeled and ^{15}N-Labeled Cu(II)–Aβ(1–16) Complexes and Dien–Cu(II)–Aβ(1–16) Complexes

Three-pulse ESEEM experiments were carried out on the equimolar mixture of Cu(II) and each of Aβ(1–16), Aβ(1–16)H6[^{15}N], Aβ(1–16)H13[^{15}N], and Aβ(1–16)H14[^{15}N] under three different conditions at pH 7.4. The normalized time-domain signals are shown in **Figure S4**.

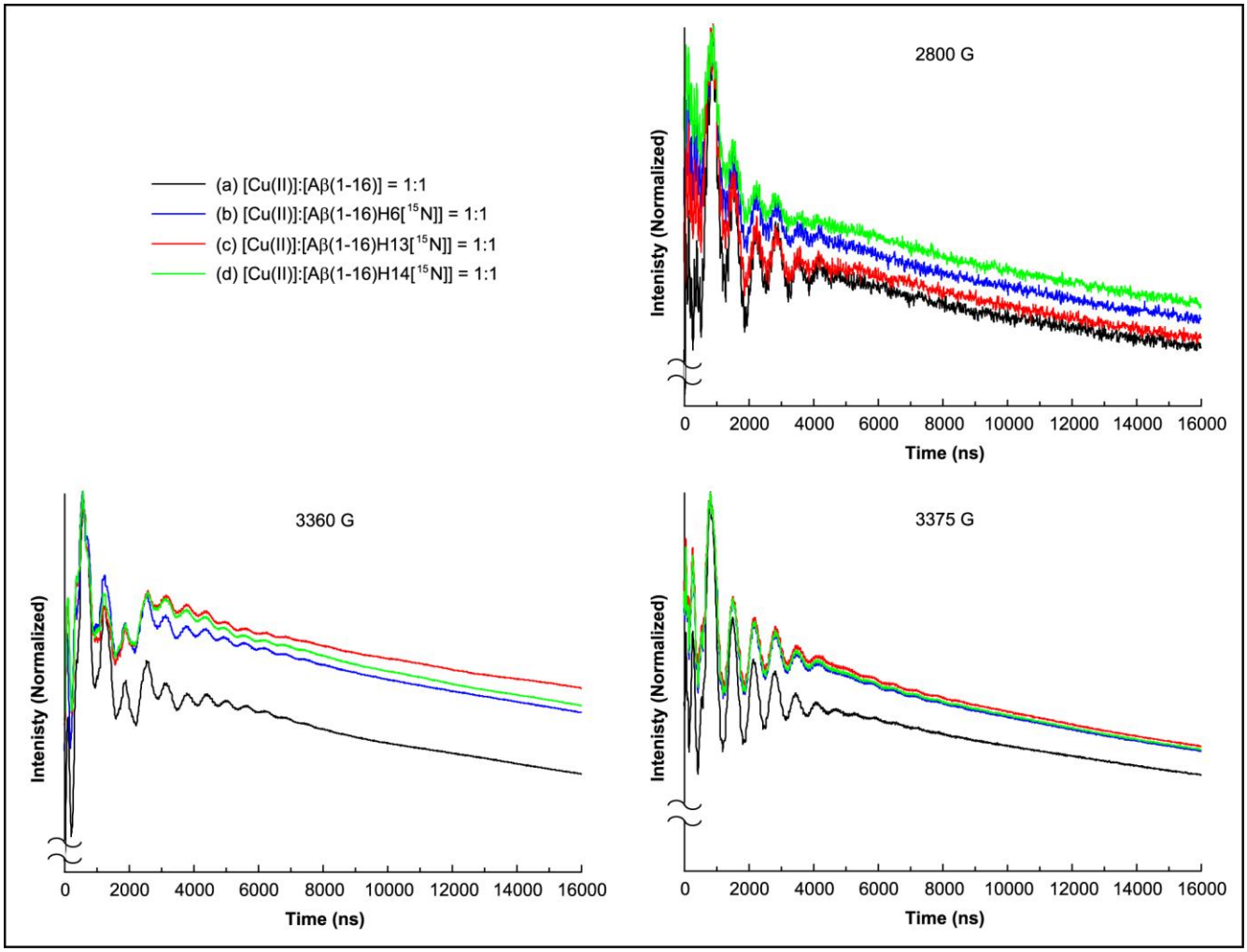

Figure S4. Three-pulse ESEEM time-domain curves of the nonlabeled and ^{15}N-labeled Aβ(1–16) analogues mixed with an equimolar amount of Cu(II) collected under three different conditions at pH 7.4. Each curve is normalized to its maximum intensity and parallel-shifted along the ordinate to fit the scale.

Three-pulse ESEEM experiments were carried out on the equimolar mixture of Cu(II) and each of Aβ(1–16), Aβ(1–16)H6[^{15}N], Aβ(1–16)H13[^{15}N], and Aβ(1–16)H14[^{15}N] under three different conditions at pH 6.0. The normalized time-domain signals are shown in **Figure S5**.

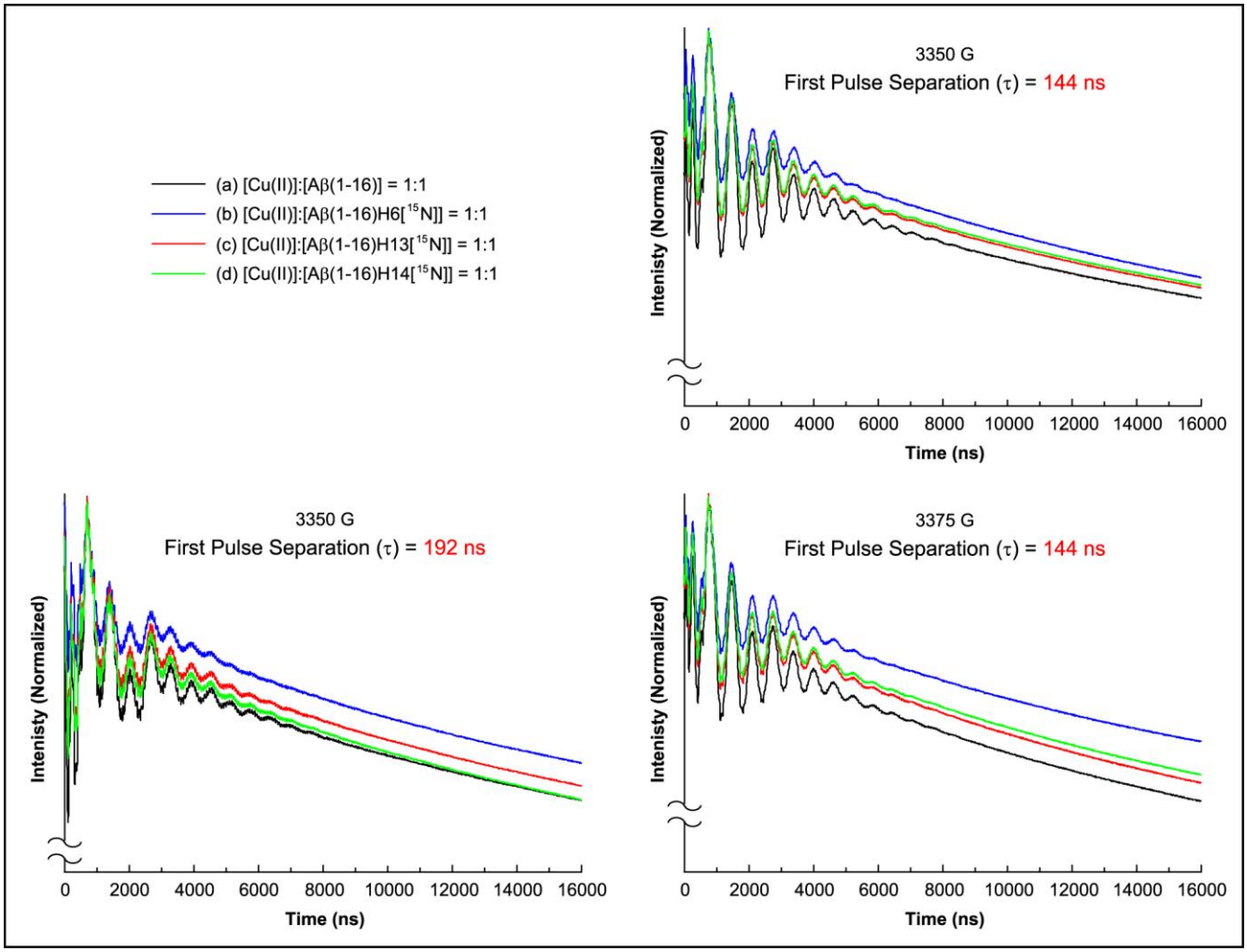

Figure S5. Three-pulse ESEEM time-domain curves of the nonlabeled and ^{15}N-labeled Aβ(1–16) analogues mixed with an equimolar amount of Cu(II) collected under three different conditions at pH 6.0. Each curve is normalized to its maximum intensity and parallel-shifted along the ordinate to fit the scale.

Three-pulse ESEEM experiments were also carried out on the equimolar mixture of the Cu(II)–dien complex and each of Aβ(1–16), Aβ(1–16)H6[^{15}N], Aβ(1–16)H13[^{15}N], and Aβ(1–16)H14[^{15}N] under two different conditions at pH 7.4. The normalized time-domain signals are shown in **Figure S6**.

The time-domain curves of the ^{15}N-labeled versions have shallower modulations than the nonlabeled counterparts, which signifies that the ^{15}N-labeled histidine residue contributes to the Cu(II) coordination.

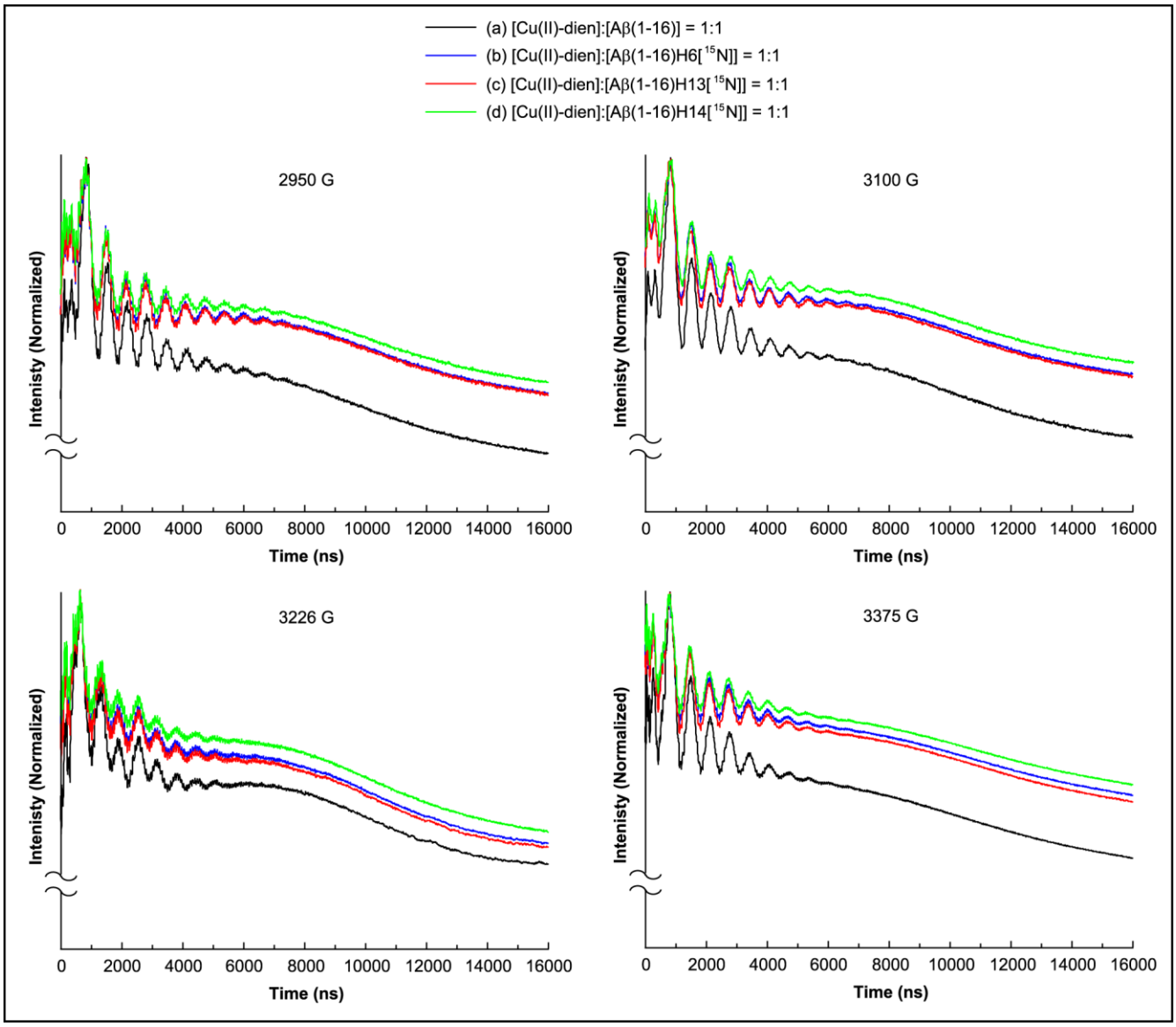

Figure S6. Three-pulse ESEEM time-domain curves of the nonlabeled and ^{15}N-labeled Aβ(1–16) analogues mixed with an equimolar amount of the Cu(II)–dien complex collected under four different conditions at pH 7.4. Each curve is normalized to its maximum intensity and parallel-shifted along the ordinate to fit the scale.

Intensities of the ^{14}N-ESEEM and ^{1}H-ESEEM Regions in the Three-Pulse ESEEM Spectra

Table S3, **Table S4**, and **Table S5** show the integrated intensities of the ESEEM spectra of the nonlabeled and ^{15}N-labeled Aβ(1–16) analogues mixed with an equimolar amount of either Cu(II) or Cu(II)–dien complex.

Table S3. Relative integrated intensities of the ESEEM spectra of the nonlabeled and ^{15}N-labeled Aβ(1–16) analogues at pH 7.4 mixed with an equimolar amount of Cu(II) at the ^{14}N-ESEEM region (0–8 MHz) and ^{1}H-ESEEM region (10–14 MHz / 12–16 MHz) and the relative contribution of each histidine residue.

	(a) ^{14}N-ESEEM	(b) ^{1}H-ESEEM	[(a) / (b)][a]	reduction[b] (%)
Cu(II) complex (2800 G; first pulse separation of 144 ns)				
Aβ(1–16)	1380 ± 8	279 ± 6	4.95 ± 0.11	0
Aβ(1–16)H6[^{15}N]	974 ± 8	302 ± 6	3.23 ± 0.06	37.1 ± 1.0
Aβ(1–16)H13[^{15}N]	1090 ± 7	271 ± 5	4.02 ± 0.08	18.8 ± 0.5
Aβ(1–16)H14[^{15}N]	801 ± 8	278 ± 6	2.88 ± 0.07	41.8 ± 1.3
Cu(II) complex (3360 G; first pulse separation of 200 ns)				
Aβ(1–16)	1590 ± 0.2	36.5 ± 0.2	43.7 ± 0.2	0
Aβ(1–16)H6[^{15}N]	1080 ± 0.2	36.1 ± 0.1	30.0 ± 0.1	31.3 ± 0.2
Aβ(1–16)H13[^{15}N]	1090 ± 0.3	36.2 ± 0.2	30.0 ± 0.2	31.2 ± 0.2
Aβ(1–16)H14[^{15}N]	1070 ± 0.3	35.1 ± 0.2	30.5 ± 0.2	30.1 ± 0.2
Cu(II) complex (3375 G; first pulse separation of 144 ns)				
Aβ(1–16)	1260 ± 0.8	90.1 ± 0.6	13.96 ± 0.09	0
Aβ(1–16)H6[^{15}N]	933 ± 0.7	107 ± 0.7	8.72 ± 0.06	37.5 ± 0.5
Aβ(1–16)H13[^{15}N]	911 ± 0.7	108 ± 0.7	8.44 ± 0.06	39.5 ± 0.5
Aβ(1–16)H14[^{15}N]	914 ± 0.7	108 ± 0.7	8.47 ± 0.06	39.3 ± 0.5

[a] Normalized ^{14}N-ESEEM intensity.

[b] Reduction in normalized ^{14}N-ESEEM intensity compared with that of the nonlabeled version; relative contribution of the ^{15}N-labeled residue to the intensity of the nonlabeled version.

Table S4. Relative integrated intensities of the ESEEM spectra of the nonlabeled and ^{15}N-labeled Aβ(1–16) analogues at pH 6.0 mixed with an equimolar amount of Cu(II) at the ^{14}N-ESEEM region (0–8 MHz) and ^{1}H-ESEEM region (12–16 MHz) and the relative contribution of each histidine residue.

	(a) ^{14}N-ESEEM	(b) ^{1}H-ESEEM	[(a) / (b)][a]	reduction[b] (%)
Cu(II) complex (3350 G; first pulse separation of 144 ns)				
Aβ(1–16)	1310 ± 0.7	77.5 ± 0.5	16.9 ± 0.2	0
Aβ(1–16)H6[^{15}N]	730 ± 0.7	79.4 ± 0.5	9.20 ± 0.06	45.4 ± 0.4
Aβ(1–16)H13[^{15}N]	981 ± 0.7	81.2 ± 0.5	12.2 ± 0.1	28.3 ± 0.3
Aβ(1–16)H14[^{15}N]	913 ± 0.7	78.1 ± 0.5	11.7 ± 0.1	30.7 ± 0.3
Cu(II) complex (3350 G; first pulse separation of 192 ns)				
Aβ(1–16)	1360 ± 0.6	162 ± 0.4	8.38 ± 0.02	0
Aβ(1–16)H6[^{15}N]	738 ± 0.6	167 ± 0.4	4.42 ± 0.01	47.2 ± 0.2
Aβ(1–16)H13[^{15}N]	1060 ± 0.6	166 ± 0.4	6.37 ± 0.02	24.0 ± 0.1
Aβ(1–16)H14[^{15}N]	1010 ± 0.6	166 ± 0.4	6.10 ± 0.02	27.3 ± 0.1
Cu(II) complex (3375 G; first pulse separation of 144 ns)				
Aβ(1–16)	1400 ± 0.9	81.3 ± 0.7	17.2 ± 0.2	0
Aβ(1–16)H6[^{15}N]	754 ± 0.8	82.8 ± 0.7	9.10 ± 0.09	47.0 ± 0.4
Aβ(1–16)H13[^{15}N]	1030 ± 0.9	81.8 ± 0.7	12.6 ± 0.1	27.0 ± 0.3
Aβ(1–16)H14[^{15}N]	1020 ± 0.9	84.3 ± 0.7	12.2 ± 0.1	29.2 ± 0.3

[a] Normalized ^{14}N-ESEEM intensity.

[b] Reduction in normalized ^{14}N-ESEEM intensity compared with that of the nonlabeled version; relative contribution of the ^{15}N-labeled residue to the intensity of the nonlabeled version.

Table S5. Relative integrated intensities of the ESEEM spectra of the nonlabeled and ^{15}N-labeled Aβ(1–16) analogues at pH 7.4 mixed with an equimolar amount of the Cu(II)–dien complex at the ^{14}N-ESEEM region (0–8 MHz) and ^{1}H-ESEEM region (10–14 MHz / 12–16 MHz) and the relative contribution of each histidine residue.

	(a) ^{14}N-ESEEM	(b) ^{1}H-ESEEM	[(a) / (b)][a]	reduction[b] (%)
Cu(II)–dien complex (2950 G; first pulse separation of 144 ns)				
Aβ(1–16)	949 ± 2	157 ± 1	6.04 ± 0.05	0
Aβ(1–16)H6[^{15}N]	665 ± 2	162 ± 2	4.10 ± 0.04	32.1 ± 0.4
Aβ(1–16)H13[^{15}N]	698 ± 2	166 ± 2	4.20 ± 0.05	30.6 ± 0.4
Aβ(1–16)H14[^{15}N]	558 ± 2	163 ± 2	3.42 ± 0.04	43.4 ± 0.6
Cu(II)–dien complex (3100 G; first pulse separation of 144 ns)				
Aβ(1–16)	840 ± 2	28.8 ± 0.9	29.2 ± 1.1	0
Aβ(1–16)H6[^{15}N]	592 ± 1	32.9 ± 0.9	18.0 ± 0.4	38.3 ± 1.7
Aβ(1–16)H13[^{15}N]	629 ± 1	33.0 ± 0.9	19.1 ± 0.5	34.6 ± 1.6
Aβ(1–16)H14[^{15}N]	508 ± 1	33.1 ± 0.9	15.4 ± 0.4	47.4 ± 2.1
Cu(II)–dien complex (3226 G; first pulse separation of 200 ns)				
Aβ(1–16)	919 ± 1	153 ± 1	5.99 ± 0.03	0
Aβ(1–16)H6[^{15}N]	648 ± 1	154 ± 1	4.20 ± 0.02	29.8 ± 0.2
Aβ(1–16)H13[^{15}N]	695 ± 1	156 ± 1	4.44 ± 0.03	25.8 ± 0.2
Aβ(1–16)H14[^{15}N]	507 ± 1	147 ± 1	3.44 ± 0.02	42.6 ± 0.3
Cu(II)–dien complex (3375 G; first pulse separation of 144 ns)				
Aβ(1–16)	673 ± 0.5	67.3 ± 0.3	10.0 ± 0.1	0
Aβ(1–16)H6[^{15}N]	515 ± 0.5	79.4 ± 0.4	6.49 ± 0.03	35.1 ± 0.2
Aβ(1–16)H13[^{15}N]	541 ± 0.5	70.5 ± 0.4	7.67 ± 0.05	23.3 ± 0.2
Aβ(1–16)H14[^{15}N]	463 ± 0.5	81 2 ± 0.5	5.70 ± 0.03	43.0 ± 0.3

[a] Normalized ^{14}N-ESEEM intensity.

[b] Reduction in normalized ^{14}N-ESEEM intensity compared with that of the nonlabeled version; relative contribution of the ^{15}N-labeled residue to the intensity of the nonlabeled version.

In each spectrum, the integrated intensity of the ^{14}N-ESEEM region between 0 and 8 MHz is normalized by that of the ^{1}H-ESEEM region either between 10 and 14 MHz or between 12 and 16 MHz. The normalized intensity decreases when ^{14}N of a histidine residue is replaced with ^{15}N. The decreases accounts for the contribution of the ^{15}N-labeled histidine residue to the ^{14}N-ESEEM signal of the nonlabeled version. While a higher contribution of the ^{15}N-labeled histidine residue to the Cu(II) coordination in the complex leads to more reduction in the normalized intensity, the correlation may not be linear. Thus, comparison between different analogues is more meaningful than absolute numbers.

Number of Histidine Residues That Simultaneously Coordinate to Cu(II) in Component I

A comparison of the ESEEM spectra of the nonlabeled Cu(II)–Aβ(1–16) complex and nonlabeled dien–Cu(II)–Aβ(1–16) complex at 3375 G provides information about the number of histidine residues simultaneously coordinating to Cu(II) in Component I. **Figure S7** shows the comparison between the ESEEM spectra of the nonlabeled Cu(II)–Aβ(1–16) complex at pH 6.0 and the nonlabeled dien–Cu(II)–Aβ(1–16) complex at pH 7.4.

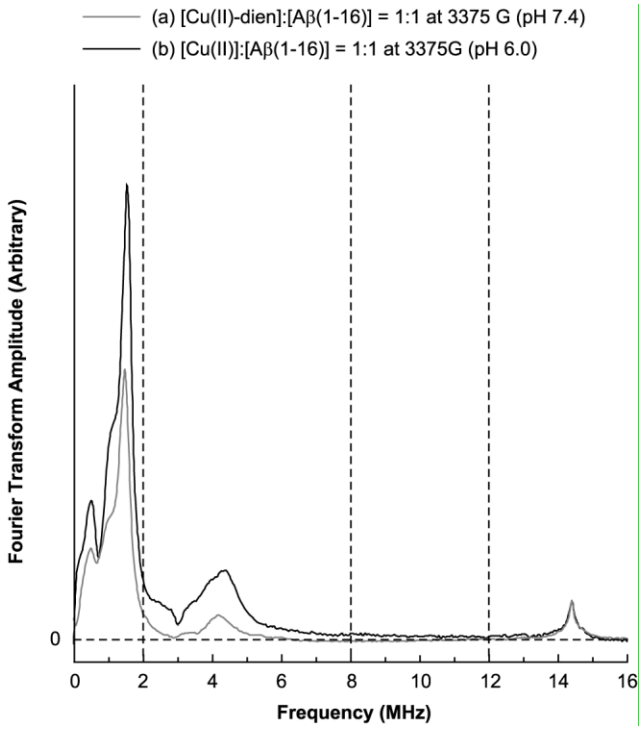

Figure S7. Comparison of the NQI region (0–2 MHz), DQ region (2–8 MHz), and ^{1}H-ESEEM region (12–16 MHz) between the ESEEM spectra of the nonlabeled Aβ(1–16) peptide mixed with an equimolar amount of Cu(II) at pH 6.0 and the nonlabeled peptide mixed with an equimolar amount of the Cu(II)–dien complexes at pH 7.4. The vertical dashed lines separate the NQI region, DQ region, and ^{1}H-ESEEM region. The ^{14}N-ESEEM intensity normalized by the ^{1}H-ESEEM intensity provides information about the number of histidine residues that simultaneously coordinate to Cu(II) in Component I.

In general, the ratio of the integrated intensity of the double-quantum region (2–8 MHz) to that of the NQI region (0–2 MHz) increases with the number of equivalent ESEEM-active ^{14}N nuclei coupled in an electron spin system.[1] The double-quantum peak is more prominent in the Cu(II)–Aβ(1–16) complex at pH 6.0 than in the dien–Cu(II)–Aβ(1–16) complex, where only one histidine residue equatorially coordinates to Cu(II) at the same time. These results indicate that more than one histidine residue simultaneously coordinate to Cu(II) in at least a fraction of Component I in the Cu(II)–Aβ(1–16) complex.

A similar approach is possible by comparing the normalized ^{14}N-ESEEM intensities with each other. Calculations reveal that the normalized ^{14}N-ESEEM intensity of the Cu(II)–Aβ(1–16) complex is approximately 1.7 times as much as that of the complex with dien, which signifies that approximately two histidine residues simultaneously coordinate to Cu(II) in Component I.

The consistent results by both approaches indicate that the normalized ^{14}N-ESEEM intensity of the ESEEM spectrum of a Cu(II) complex can provide critical information about the number of equivalent ^{14}N nuclei coupled to an electron spin system when the ESEEM spectrum of a ternary Cu(II) complex with a tridentate ligand such as dien is used as a reference.

Table S6 shows the integrated intensities of the ESEEM spectrum of the nonlabeled Aβ(1–16) peptide mixed with an equimolar amount of Cu(II) at pH 6.0 and that of the nonlabeled Aβ(1–16) mixed with an equimolar amount of the Cu(II)–dien complex at pH 7.4. The two spectra have almost identical spectral shapes including peak positions in the ^{14}N-ESEEM region below 8 MHz and in the ^{1}H-ESEEM region around 14.4 MHz. The similarity in the peak shapes implies that the ESEEM-active nuclei of both complexes have almost identical nuclear transition frequencies.

Table S6. Comparison of the ESEEM spectrum of the nonlabeled Aβ(1−16) peptide mixed with an equimolar amount of Cu(II) at pH 6.0 and that of the nonlabeled Aβ(1−16) mixed with an equimolar amount of the Cu(II)−dien complex at pH 7.4. Both spectra were obtained at 3375 G with a first pulse separation of 144 ns. The integrated intensities of the ^{14}N-ESEEM region (0–8 MHz), which includes the NQI region (0–2 MHz) and the DQ region (2–8 MHz), and the ^{1}H-ESEEM region (12–16 MHz) are compared with one another.

	^{14}N-ESEEM region (0–8 MHz) and ^{1}H-ESEEM region (12–16 MHz)			
	(a) ^{14}N-ESEEM	(b) ^{1}H-ESEEM	[(a) / (b)][a]	(1) / (2)
Cu(II)–Aβ	1400 ± 0.9	81.3 ± 0.7	(1) 17.2 ± 0.2	1.7
dien–Cu(II)–Aβ	673 ± 0.5	67.3 ± 0.3	(2) 10.0 ± 0.1	
	NQI ^{14}N-ESEEM region (0–2 MHz) and DQ ^{14}N-ESEEM region (2–8 MHz)			
	(c) NQI region	(d) DQ region	(d) / (c)	(3) / (4)
Cu(II)–Aβ	943 ± 0.5	457 ± 0.8	(3) 0.49 ± 0.01	2.5
dien–Cu(II)–Aβ	560 ± 0.3	113 ± 0.4	(4) 0.20 ± 0.01	

[a] Normalized ^{14}N-ESEEM intensity.

HYSCRORE Spectra of the Dien–Cu(II)–A*β*(1–16) Complexes

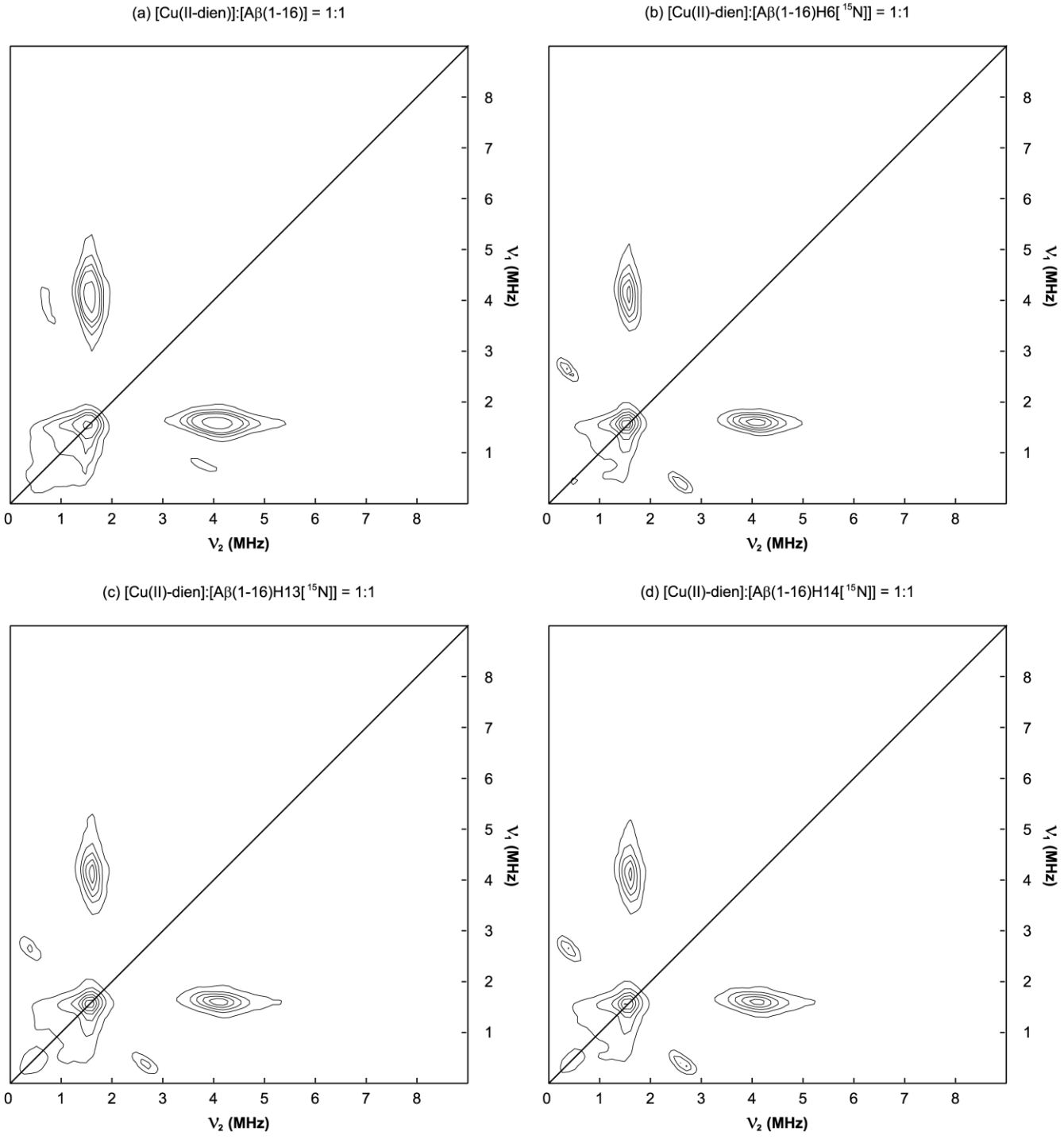

Figure S8. HYSCORE spectra of the nonlabeled and ^{15}N-labeled A*β*(1–16) analogues mixed with an equimolar amount of the Cu(II)–dien complex. The cross-peak around (1.6 MHz, 4.0 MHz) is assigned to the correlation between ^{14}N transition frequencies and the cross-peak around (0.4 MHz, 2.6 MHz) is due to the correlation bewteen ^{15}N transition frequencies.

Four-pulse hyperfine sublevel correlation (HYSCORE) experiments were carried out on the equimolar mixture of the Cu(II)–dien complex and each of Aβ(1−16), Aβ(1−16)H6[^{15}N], Aβ(1−16)H13[^{15}N], and Aβ(1−16)H14[^{15}N] at 3375 G. **Figure S8** shows the HYSCORE spectra of the mixtures as the contour plots of the magnitude of the two-dimensional Fourier transforms. Each of the four spectra has a cross-peak around (1.6 MHz, 4.0 MHz), which is assigned to the correlation between ^{14}N transition frequencies. Also, each of the three spectra of the ^{15}N-labeled analogues has a cross-peak around (0.4 MHz, 2.6 MHz), which is due to the correlation between ^{15}N transition frequencies.

Three-Pulse ESEEM Simulation

The experimentally obtained three-pulse ESEEM spectra of the nonlabeled Aβ(1−16) peptide mixed with an equimolar amount of Cu(II) or the Cu(II)−dien complex were fitted to simulated spectra. In the simulations, the g-tensor of the electron spin and the hyperfine tensor of the ^{14}N nuclear spin were assumed to be isotropic and axially symmetric, respectively. Accordingly, only two Euler angles between the nuclear quadrupole tensor and the hyperfine tensor, α and β, were varied. The NQI parameters for the two components are assumed to be almost identical.

Two equivalent ESEEM-active ^{14}N nuclei and one ESEEM-active ^{14}N nucleus were assumed to be coupled to the Cu(II) electron spin system in Component I and Component II, respectively. With methods provided by researchers,[2–5] the best fits were obtained by assuming 75% Component I and 25% Component II for the simulation of each of the Cu(II)−Aβ(1−16) spectra obtained at 3360 G and 3375 G. With the ESEEM parameters, the ESEEM spectrum obtained at 2800 G appears to be accounted for solely by Component I in our spectral simulations even though some noticeable differences in frequency are seen due to the low signal-to-noise ratio and possible orientation selectivity around the $g_{||}$ region. Also, the ESEEM parameters of Component I were used for the simulations of the dien−Cu(II)−Aβ(1−16) spectra. The ESEEM parameters used for the simulations are shown in **Table S7**.

Table S7. Parameters used for the simulations of the three-pulse ESEEM spectra of the nonlabeled Aβ(1–16) peptide mixed with an equimolar amount of Cu(II) or the Cu(II)–dien complex.

	NQI parameters		
	e^2qQ/h (MHz)		η
Component I	1.70 ± 0.03		0.65 ± 0.02
Component II	1.70 ± 0.03		0.65 ± 0.02
	hyperfine parameters		
	A_{iso} (MHz)		$\lvert T \rvert$ (MHz)
Component I	1.87 ± 0.04		0.12 ± 0.01
Component II	1.71 ± 0.04		0.11 ± 0.01
	Euler angles		
	α (°)	β (°)	γ (°)
Component I	75 / 255 ± 5	75 ± 5	0 (fixed)
Component II	90 ± 5	90 ± 5	0 (fixed)

Figure S9 illustrates the experimentally obtained spectra overlaid with the corresponding simulated spectra.

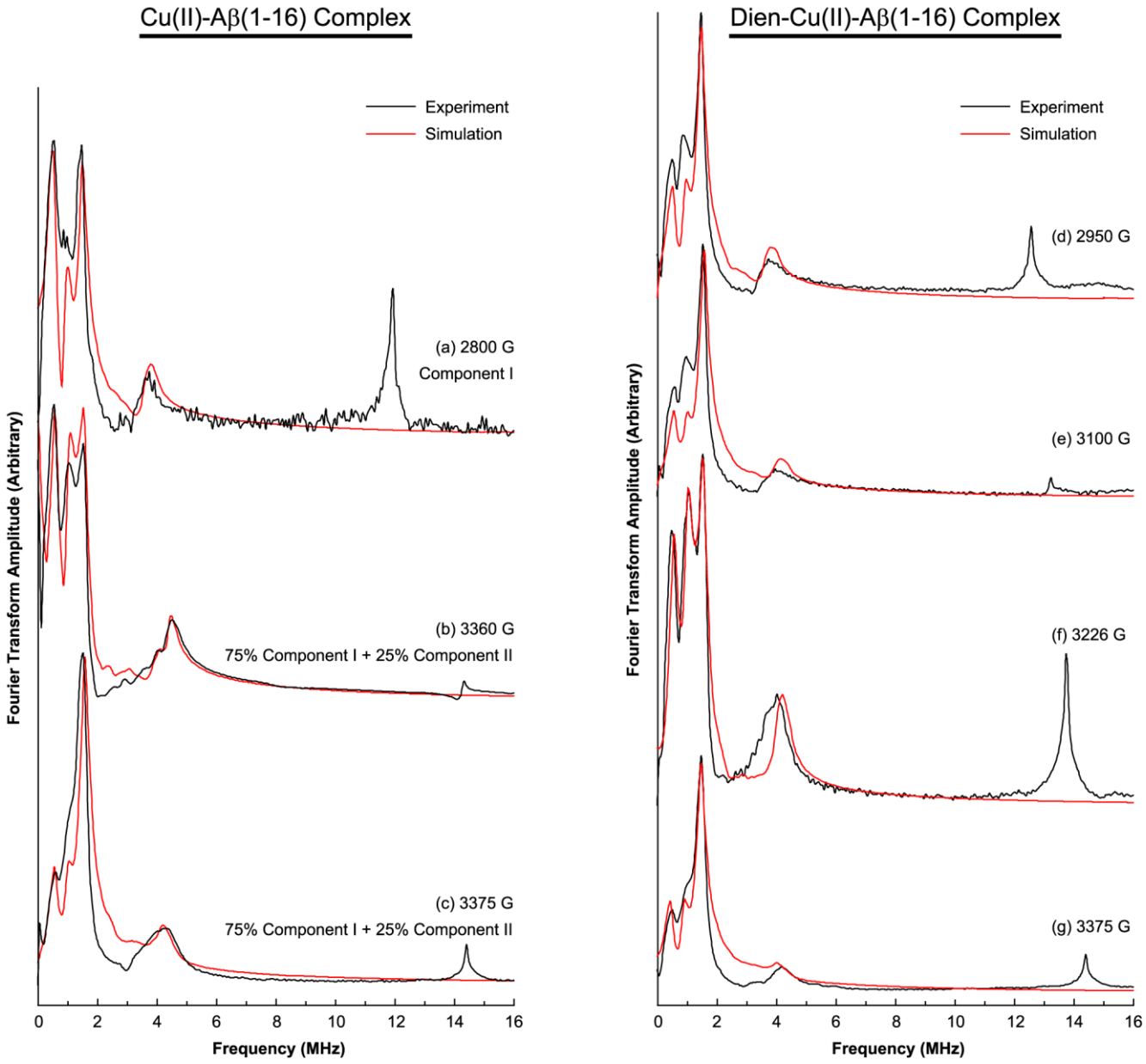

Figure S9. Experimentally obtained and simulated three-pulse ESEEM spectra of the nonlabeled Aβ(1−16) peptide mixed with an equimolar amount of Cu(II) or the Cu(II)−dien complex.

Appendix: Change in the Modulation Depths of the ^{14}N Frequencies by a Replacement of ^{14}N with ^{15}N

(1) Relative modulation depth (Case I: one nitrogen coupled to an electron spin system)

For a system with an electron spin of one half, the three-pulse ESEEM time-domain signal obtained by a conventional stimulated-echo pulse sequence of $\pi/2-\tau-\pi/2-T-\pi/2-\tau-$ echo is given by:[4]

$$V(\tau, T) = \frac{1}{2}\left[V^{\alpha}(\tau, T) + V^{\beta}(\tau, T)\right] \qquad \text{[S-1]}$$

where the signal in the α electron spin manifold is expressed as:

$$V^{\alpha}(\tau, T) = 1 - \frac{k}{2}(1 - \cos\omega_{\beta}\tau)[1 - \cos\omega_{\alpha}(\tau + T)] \qquad \text{[S-2]}$$

The constant k is the modulation depth parameter, and ω_{α} and ω_{β} are the nuclear spin transition frequency in the α and β electron spin manifold, respectively. The signal in the β electron spin manifold can be expressed in the same fashion. Introducing new symbols, one can simplify eq [S-2].[6]

$$\begin{aligned} V^{\alpha}(\tau, T) &= 1 - K^{\alpha}(1 - S^{\alpha}) \\ &= 1 - K^{\alpha} + K^{\alpha}S^{\alpha} \end{aligned} \qquad \text{[S-3]}$$

where

$$K^{\alpha}(\tau) = \frac{k}{2}(1 - \cos\omega_{\beta}\tau) \qquad \text{[S-4]}$$

$$S^{\alpha}(\tau, T) = \cos\omega_{\alpha}(\tau + T) \qquad \text{[S-5]}$$

In eq [S-3] the first two terms are the zero-frequency part, which is independent of T, while the last term is the oscillating part. When two or more nuclear spins are considered in the same electron spin system, the ESEEM signal is expressed by the product rule.[4,5]

$$V(\tau, T) = \frac{1}{2}\left[\prod_{i=1}^{N} V_i^{\alpha}(\tau, T) + \prod_{i=1}^{N} V_i^{\beta}(\tau, T)\right] \quad (i = 1, 2, 3, \cdots, N) \qquad \text{[S-6]}$$

where $V_i^{\alpha}(\tau, T)$ and $V_i^{\beta}(\tau, T)$ are the contribution of the *i*th nuclear spin to the total signal in the α and β electron spin manifold, respectively, and N is the number of coupled nuclei. If one ^{14}N nuclear spin and one ^{1}H nuclear spin are coupled to an electron spin, the total signal is:

$$V_{14,1}(\tau, T) = \frac{1}{2}\Big[V_{14}^{\alpha}(\tau, T)V_1^{\alpha}(\tau, T) + V_{14}^{\beta}(\tau, T)V_1^{\beta}(\tau, T)\Big] \quad \text{[S-7]}$$

where the subscripts 14 and 1 denote the ^{14}N spin and the ^{1}H spin, respectively. For a weakly coupled ^{1}H nucleus, $V_1^{\alpha}(\tau, T)$ and $V_1^{\beta}(\tau, T)$ are almost identical, which leads to a deeper modulation at one frequency. Then, using eq [S-3], one can rewrite eq [S-7] as:

$$V_{14,1}(\tau, T) = \frac{1}{2}\Big[(1 - K_{14}^{\alpha} + K_{14}^{\alpha}S_{14}^{\alpha}) + (1 - K_{14}^{\beta} + K_{14}^{\beta}S_{14}^{\beta})\Big](1 - K_1 + K_1S_1) \quad \text{[S-8]}$$

where

$$K_1 = K_1^{\alpha} = K_1^{\beta} \quad \text{[S-9]}$$

$$S_1 = S_1^{\alpha} = S_1^{\beta} \quad \text{[S-10]}$$

Expansion of eq [S-8] gives an equation that contains the zero-frequency part and the oscillating part with several different frequencies.

$$V_{14,1}(\tau, T) = A + BS_{14}^{\alpha} + CS_{14}^{\beta} + DS_1 + ES_{14}^{\alpha}S_1 + FS_{14}^{\beta}S_1 \quad \text{[S-11]}$$

where

$$A = \Big(1 - \frac{K_{14}^{\alpha} + K_{14}^{\beta}}{2}\Big)(1 - K_1) \quad \text{[S-12]}$$

$$B = \frac{K_{14}^{\alpha}(1 - K_1)}{2} \quad \text{[S-13]}$$

$$C = \frac{K_{14}^{\beta}(1 - K_1)}{2} \quad \text{[S-14]}$$

$$D = K_1\Big(1 - \frac{K_{14}^{\alpha} + K_{14}^{\beta}}{2}\Big) \quad \text{[S-15]}$$

$$E = \frac{K_{14}^{\alpha}K_1}{2} \quad \text{[S-16]}$$

$$F = \frac{K^{\beta}_{14} K_1}{2} \qquad \text{[S-17]}$$

The first term is the zero-frequency part, the second and third terms are the oscillations due to the ^{14}N nuclear spin, the four term is the oscillation due to the ^{1}H nucleus. The fifth and sixth terms are the oscillations due to the combination of the two nuclear spins. It is straightforward that the modulation depths of the second, third, and fourth term are proportional to their coefficients, B, C, and D, respectively. Particularly, the ratio of B to D is expressed as:

$$B/D = \frac{K^{\alpha}_{14}(1 - K_1)}{K_1(2 - K^{\alpha}_{14} - K^{\beta}_{14})} \qquad \text{[S-18]}$$

The ratio B/D is the relative modulation depth of an ^{14}N nuclear transition frequency in the α electron spin manifold, which is normalized by that of the ^{1}H transition frequency. Similarly, the ratio C/D is the relative modulation depth of the corresponding transition frequency in the β electron spin manifold.

(2) Relative modulation depth (Case II: two equivalent nitrogen nuclei)

In the case that two equivalent ^{14}N nuclear spins and one ^{1}H nuclear spin are coupled to the same electron spin, the total signal becomes:

$$V_{14,14,1}(\tau, T) = \frac{1}{2}\Big[[V^{\alpha}_{14}(\tau, T)]^2 V^{\alpha}_{1}(\tau, T) + [V^{\beta}_{14}(\tau, T)]^2 V^{\beta}_{1}(\tau, T)\Big] \qquad \text{[S-19]}$$

Then, [S-19] can be rewritten in the same manner as eq [S-7].

$$V_{14,14,1}(\tau, T) = \frac{1}{2}\Big[(1 - K^{\alpha}_{14} + K^{\alpha}_{14} S^{\alpha}_{14})^2 + (1 - K^{\beta}_{14} + K^{\beta}_{14} S^{\beta}_{14})^2\Big](1 - K_1 + K_1 S_1) \qquad \text{[S-20]}$$

Like eq [S-8], expansion of eq [S-20] gives an equation that contains the zero-frequency part and the oscillating part. The coefficient of the term containing S^{α}_{14}, B_2, is expressed as:

$$B_2 = K^{\alpha}_{14}(1 - K^{\alpha}_{14})(1 - K_1) \qquad \text{[S-21]}$$

where the subscript 2 denotes two equivalent ^{14}N spins. Considering the fact that $(S^{\alpha}_{14})^2$ and $(S^{\beta}_{14})^2$ contribute to the zero-frequency part, one can also calculate the coefficient of the term containing S_1, D_2.

$$D_2 = \frac{K_1}{4}\left[2\,(1-K^{\alpha}_{14})^2 + (K^{\alpha}_{14})^2 + 2\,(1-K^{\beta}_{14})^2 + (K^{\beta}_{14})^2\right] \qquad \text{[S-22]}$$

Finally, the ratio of B_2 to D_2 is expressed as:

$$B_2/D_2 = \frac{4K^{\alpha}_{14}(1-K^{\alpha}_{14})(1-K_1)}{K_1\left[2\,(1-K^{\alpha}_{14})^2 + (K^{\alpha}_{14})^2 + 2\,(1-K^{\beta}_{14})^2 + (K^{\beta}_{14})^2\right]} \qquad \text{[S-23]}$$

The ratios B/D and B_2/D_2 represent the relative modulation depth of an ^{14}N nuclear transition frequency in the α electron spin manifold, which is normalized by that of the ^{1}H transition frequency in the case of one and two coupled ^{14}N, respectively. The relative modulation depth of the ^{14}N nuclear transition frequency increases with an additional ^{14}N nucleus and the factor of increase is given by:

$$F(2\ ^{14}\mathrm{N}/1\ ^{14}\mathrm{N}) = \frac{B_2/D_2}{B/D} = \frac{4(1-K^{\alpha}_{14})(2-K^{\alpha}_{14}-K^{\beta}_{14})}{2\,(1-K^{\alpha}_{14})^2 + (K^{\alpha}_{14})^2 + 2\,(1-K^{\beta}_{14})^2 + (K^{\beta}_{14})^2} \qquad \text{[S-24]}$$

If K^{α}_{14} and K^{β}_{14} are much smaller than 1, the factor converges to 2.

Next, if one of the two ^{14}N nuclei is replaced with ^{15}N, the coupled nuclei in the electron spin system are one ^{14}N nuclear spin, one ^{15}N nuclear spin, and one ^{1}H nuclear spin. Then, the total signal becomes:

$$V_{14,15,1}(\tau,\,T) = \frac{1}{2}\left[V^{\alpha}_{14}(\tau,\,T)\,V^{\alpha}_{15}(\tau,\,T)\,V^{\alpha}_{1}(\tau,\,T) + V^{\beta}_{14}(\tau,\,T)\,V^{\beta}_{15}(\tau,\,T)\,V^{\beta}_{1}(\tau,\,T)\right] \qquad \text{[S-25]}$$

where the subscript 15 denotes the ^{15}N spin. In the case that the modulation of ^{15}N is significantly shallower than that of ^{14}N and ^{1}H, V^{α}_{15} and V^{β}_{15} are almost 1. Thus, the time-domain signal appears as if one ^{14}N and one ^{1}H nuclear spin were coupled.

$$V_{14,15,1}(\tau,\,T) \approx \frac{1}{2}\left[V^{\alpha}_{14}(\tau,\,T)\,V^{\alpha}_{1}(\tau,\,T) + V^{\beta}_{14}(\tau,\,T)\,V^{\beta}_{1}(\tau,\,T)\right] = V_{14,1}(\tau,\,T) \qquad \text{[S-26]}$$

(3) Relative modulation depth (Case III: two non-equivalent nitrogen nuclei)

In the case that two non-equivalent ^{14}N nuclear spins and one ^{1}H nuclear spin are coupled to the same electron spin, the total signal becomes:

$$V_{14,14',1}(\tau, T) = \frac{1}{2}\Big[V^{\alpha}_{14}(\tau, T)\, V^{\alpha}_{14'}(\tau, T)\, V^{\alpha}_{1}(\tau, T) + V^{\beta}_{14}(\tau, T)\, V^{\beta}_{14'}(\tau, T)\, V^{\beta}_{1}(\tau, T)\Big] \quad \text{[S-27]}$$

where the subscripts 14 and 14' denote two distinguishable ^{14}N spins. Then, [S-27] can be rewritten in the same manner as eqs [S-7] and [S-19].

$$V_{14,14',1}(\tau, T) = \frac{1}{2}(1 - K_1 + K_1 S_1)$$
$$\Big[(1 - K^{\alpha}_{14} + K^{\alpha}_{14} S^{\alpha}_{14})(1 - K^{\alpha}_{14'} + K^{\alpha}_{14'} S^{\alpha}_{14'}) + (1 - K^{\beta}_{14} + K^{\beta}_{14} S^{\beta}_{14})(1 - K^{\beta}_{14'} + K^{\beta}_{14'} S^{\beta}_{14'})\Big] \quad \text{[S-28]}$$

Like eqs [S-8] and [S-20], expansion of eq [S-28] gives an equation that contains the zero-frequency part and the oscillating part. The sum of the coefficients of the terms containing either S^{α}_{14} or $S^{\alpha}_{14'}$, $B_{2'}$, is expressed as:

$$B_{2'} = \frac{1}{2}(K^{\alpha}_{14} + K^{\alpha}_{14'} - 2K^{\alpha}_{14} K^{\alpha}_{14'})(1 - K_1) \quad \text{[S-29]}$$

where the subscript 2' denotes two distinguishable ^{14}N spins. One can also calculate the coefficient of the term containing S_1, $D_{2'}$.

$$D_{2'} = \frac{K_1}{2}\Big[(1 - K^{\alpha}_{14})(1 - K^{\alpha}_{14'}) + (1 - K^{\beta}_{14})(1 - K^{\beta}_{14'})\Big] \quad \text{[S-30]}$$

Finally, the ratio of $B_{2'}$ to $D_{2'}$ is expressed as:

$$B_{2'}/D_{2'} = \frac{(K^{\alpha}_{14} + K^{\alpha}_{14'} - 2K^{\alpha}_{14} K^{\alpha}_{14'})(1 - K_1)}{K_1[(1 - K^{\alpha}_{14})(1 - K^{\alpha}_{14'}) + (1 - K^{\beta}_{14})(1 - K^{\beta}_{14'})]} \quad \text{[S-31]}$$

The ratio $B_{2'}/D_{2'}$ represents the sum of the relative modulation depths of the transition frequencies of the two non-equivalent ^{14}N nuclei in the α electron spin manifold, which is normalized by the

modulation depth of the ^{1}H transition frequency. The sum of the relative modulation depths, $B_{2'}/D_{2'}$, is greater than B/D, the relative modulation depth of the ^{14}N nuclear transition frequency in the case of one coupled ^{14}N. The ratio of $B_{2'}/D_{2'}$ to B/D is given by:

$$\begin{aligned} F(2'\ {}^{14}\mathrm{N}/1\ {}^{14}\mathrm{N}) &= \frac{B_{2'}/D_{2'}}{B/D} \\ &= \frac{(K^{\alpha}_{14} + K^{\alpha}_{14'} - 2K^{\alpha}_{14}K^{\alpha}_{14'})(2 - K^{\alpha}_{14} - K^{\beta}_{14})}{K^{\alpha}_{14}[(1 - K^{\alpha}_{14})(1 - K^{\alpha}_{14'}) + (1 - K^{\beta}_{14})(1 - K^{\beta}_{14'})]} \end{aligned} \qquad \text{[S-32]}$$

where 2' denotes two non-equivalent ^{14}N spins. If K^{α}_{14}, $K^{\alpha}_{14'}$, K^{β}_{14}, and$K^{\beta}_{14'}$ are much smaller than 1, eq [S-32] becomes:

$$F(2'\ {}^{14}\mathrm{N}/1\ {}^{14}\mathrm{N}) = 1 + \frac{K^{\alpha}_{14'}}{K^{\alpha}_{14}} \qquad \text{[S-33]}$$

Therefore, in the case of two non-equivalent ^{14}N nuclear spins and one ^{1}H nuclear spin coupled to the same electron spin system, a comparison of relative modulations depths, which is similar to that made in the case of two equivalent ^{14}N nuclear spins, is still meaningful when the modulation depths of the different frequencies are considered together. Particularly, if K^{α}_{14} and $K^{\alpha}_{14'}$ in eq [S-33] are identical, the ratio becomes 2.

(4) Decrease in the relative modulation depth (Case I: one nitrogen nucleus)

In a system where one ^{14}N nuclear spin and one ^{1}H nuclear spin are coupled to the electron spin, if a fraction of ^{14}N is replaced with ^{15}N, the signal becomes:

$$V^{m}_{14,15,1}(\tau, T) = m\, V_{15,1}(\tau, T) + (1 - m)\, V_{14,1}(\tau, T) \qquad \text{[S-34]}$$

where m is the fraction of ^{14}N substituted with ^{15}N and

$$V_{14,1}(\tau, T) = \frac{1}{2}\Big[V^{\alpha}_{14}(\tau, T)\, V^{\alpha}_{1}(\tau, T) + V^{\beta}_{14}(\tau, T)\, V^{\beta}_{1}(\tau, T)\Big] \qquad \text{[S-35]}$$

$$V_{15,1}(\tau, T) = \frac{1}{2}\Big[V^{\alpha}_{15}(\tau, T)\, V^{\alpha}_{1}(\tau, T) + V^{\beta}_{15}(\tau, T)\, V^{\beta}_{1}(\tau, T)\Big] \quad \text{[S-36]}$$

Assuming that V^{α}_{15} and V^{β}_{15} are almost 1, one can rewrite eq [S-36] as:

$$\begin{aligned} V_{15,1}(\tau, T) &= \frac{1}{2}\Big[V^{\alpha}_{1}(\tau, T) + V^{\beta}_{1}(\tau, T)\Big] \\ &= 1 - K_1 + K_1 S_1 \end{aligned} \quad \text{[S-37]}$$

Similarly, eq [S-35] can be expressed in terms of K^{α}_{14}, S^{α}_{14}, K^{β}_{14}, and S^{β}_{14}. Thus, expansion of eq [S-34] gives an equation that contains the zero-frequency part and the oscillating part. The coefficient of the term containing S^{α}_{14}, $B^{m}_{14\text{–}15}$, is:

$$B^{m}_{14\text{–}15} = \frac{(1-m)K^{\alpha}_{14}(1-K_1)}{2} \quad \text{[S-38]}$$

where the subscript 14–15 denotes the replacement of ^{14}N with ^{15}N. Also, the coefficient of the term containing S_1, $D^{m}_{14\text{–}15}$, is:

$$D^{m}_{14\text{–}15} = K_1\Big[1 - \frac{(1-m)(K^{\alpha}_{14} + K^{\beta}_{14})}{2}\Big] \quad \text{[S-39]}$$

The ratio of $B^{m}_{14\text{–}15}$ to $B^{m}_{14\text{–}15}$ is expressed as:

$$B^{m}_{14\text{–}15}/D^{m}_{14\text{–}15} = \frac{(1-m)K^{\alpha}_{14}(1-K_1)}{K_1[2-(1-m)(K^{\alpha}_{14} + K^{\beta}_{14})]} \quad \text{[S-40]}$$

Finally, one can calculate the decrease in the relative modulation depth of the ^{14}N nuclear transition frequency by comparing $B^{m}_{14\text{–}15}/D^{m}_{14\text{–}15}$ with $B^{0}_{14\text{–}15}/D^{0}_{14\text{–}15}$, that is, B/D in eq [S-18].

$$F(m\ ^{15}\mathrm{N}/0\ ^{15}\mathrm{N}) = \frac{B^{m}_{14\text{–}15}/D^{m}_{14\text{–}15}}{B/D} = \frac{(1-m)[2-(K^{\alpha}_{14} + K^{\beta}_{14})]}{2-(1-m)(K^{\alpha}_{14} + K^{\beta}_{14})} \quad \text{[S-41]}$$

It is evident that the decrease in the relative modulation depth of the ^{14}N nuclear transition frequency is greater than that in the fraction of ^{14}N. If K^{α}_{14} and K^{β}_{14} are much smaller than 1, the factor converges to

$1 - m$, which is the fraction of ^{14}N. For example, if the K^{α}_{14} and K^{β}_{14} values are approximately 0.15, eq [S-41] becomes:

$$F(m\ ^{15}\mathrm{N}/0\ ^{15}\mathrm{N}) = \frac{1.70\,(1-m)}{1.70 + 0.30\,m} \qquad \text{[S-42]}$$

In the case of a 33% replacement of ^{14}N with ^{15}N, the ratio $F(m\ ^{15}\mathrm{N}/0\ ^{15}\mathrm{N})$ is approximately 0.63, which indicates that the relative modulation depth of the ^{14}N transition frequency decreases by 37%, 4% greater than expected from the fraction of replacement.

(5) Decrease in the relative modulation depth (Case II: two equivalent nitrogen nuclei)

One may consider another system where two equivalent ^{14}N nuclear spins and one ^{1}H nuclear spin are coupled to the same electron spin. If a fraction of either ^{14}N is replaced with ^{15}N, the signal becomes:

$$V^{n}_{14,\,14,\,15,\,1}(\tau,\,T) = n\,V_{14,\,15,\,1}\,(\tau,\,T) + (1-n)\,V_{14,\,14,\,1}(\tau,\,T) \qquad \text{[S-43]}$$

where n is the fraction of ^{14}N substituted with ^{15}N and

$$V_{14,\,14,\,1}(\tau,\,T) = \frac{1}{2}\Big[[V^{\alpha}_{14}(\tau,\,T)]^2\,V^{\alpha}_{1}(\tau,\,T) + [V^{\beta}_{14}(\tau,\,T)]^2\,V^{\beta}_{1}(\tau,\,T)\Big] \qquad \text{[S-44]}$$

$$V_{14,\,15,\,1}(\tau,\,T) = \frac{1}{2}\Big[V^{\alpha}_{14}(\tau,\,T)\,V^{\alpha}_{15}(\tau,\,T)\,V^{\alpha}_{1}(\tau,\,T) + V^{\beta}_{14}(\tau,\,T)\,V^{\beta}_{15}(\tau,\,T)\,V^{\beta}_{1}(\tau,\,T)\Big] \qquad \text{[S-45]}$$

Assuming that V^{α}_{15} and V^{β}_{15} are almost 1, one can rewrite eq [S-45] as:

$$V_{14,\,15,\,1}(\tau,\,T) = \frac{1}{2}\Big[V^{\alpha}_{14}(\tau,\,T)\,V^{\alpha}_{1}(\tau,\,T) + V^{\beta}_{14}(\tau,\,T)\,V^{\beta}_{1}(\tau,\,T)\Big] \qquad \text{[S-46]}$$

Expansion of eq [S-43] gives an equation that contains the zero-frequency part and the oscillating part. The coefficient of the term containing S^{α}_{14}, $B^{n}_{14\text{–}15}$, is:

$$B^{n}_{14\text{–}15} = \frac{K^{\alpha}_{14}(1-K_1)}{2}\Big[2(1-n)(1-K^{\alpha}_{14}) + n\Big] \qquad \text{[S-47]}$$

Also, the coefficient of the term containing S_1, $D^{n}_{14\text{–}15}$, is:

$$D^{n}{}_{14\text{–}15} = \frac{K_1}{4}\Big[3(1-n)[(K^{\alpha}_{14})^2 + (K^{\beta}_{14})^2] + 2(n-2)(K^{\alpha}_{14} + K^{\beta}_{14}) + 4\Big] \qquad \text{[S-48]}$$

The ratio of $B^{n}{}_{14\text{–}15}$ to $D^{n}{}_{14\text{–}15}$ is expressed as:

$$B^{n}{}_{14\text{–}15}/D^{n}{}_{14\text{–}15} = \frac{2K^{\alpha}_{14}(1-K_1)[2(1-n)(1-K^{\alpha}_{14}) + n]}{K_1\big[3(1-n)[(K^{\alpha}_{14})^2 + (K^{\beta}_{14})^2] + 2(n-2)(K^{\alpha}_{14} + K^{\beta}_{14}) + 4\big]} \qquad \text{[S-49]}$$

As already shown in eq [S-41], one can calculate the decrease in the relative modulation depth of the ^{14}N nuclear transition frequency by comparing $B^{n}{}_{14\text{–}15}/D^{n}{}_{14\text{–}15}$ with $B^{0}{}_{14\text{–}15}/D^{0}{}_{14\text{–}15}$, that is, B_2/D_2 in eq [S-23].

$$\begin{aligned} F(n\ {}^{15}\mathrm{N}/0\ {}^{15}\mathrm{N}) &= \frac{B^{n}{}_{14\text{–}15}/D^{n}{}_{14\text{–}15}}{B_2/D_2} \\ &= \frac{[2(1-n)(1-K^{\alpha}_{14}) + n]\big[3[(K^{\alpha}_{14})^2 + (K^{\beta}_{14})^2] - 4(K^{\alpha}_{14} + K^{\beta}_{14}) + 4\big]}{2(1-K^{\alpha}_{14})\big[3(1-n)[(K^{\alpha}_{14})^2 + (K^{\beta}_{14})^2] + 2(n-2)(K^{\alpha}_{14} + K^{\beta}_{14}) + 4\big]} \end{aligned} \qquad \text{[S-50]}$$

If n is 1, eq [S-50] becomes:

$$F(1\ {}^{15}\mathrm{N}/0\ {}^{15}\mathrm{N}) = \frac{2\,(1-K^{\alpha}_{14})^2 + (K^{\alpha}_{14})^2 + 2\,(1-K^{\beta}_{14})^2 + (K^{\beta}_{14})^2}{4(1-K^{\alpha}_{14})(2-K^{\alpha}_{14}-K^{\beta}_{14})} \qquad \text{[S-51]}$$

In fact, the right-hand side of eq [S-51] is the reciprocal of eq [S-24], which explains the increase in the relative modulation depth of the ^{14}N nuclear transition frequency with an additional ^{14}N nucleus. On the other hand, if K^{α}_{14} and K^{β}_{14} are much smaller than 1, the factor converges to $1-(n/2)$, which is the fraction of ^{14}N. If the K^{α}_{14} and K^{β}_{14} values are approximately 0.15, eq [S-50] becomes:

$$F(n\ {}^{15}\mathrm{N}/0\ {}^{15}\mathrm{N}) = \frac{2.94\,(1-0.70\,n)}{1.70\,(2.94+0.47\,n)} \qquad \text{[S-52]}$$

In the case that two-thirds of either ^{14}N is replaced with ^{15}N, the ratio $F(n\ {}^{15}\mathrm{N}/0\ {}^{15}\mathrm{N})$ is approximately 0.66, which indicates that the relative modulation depth of the ^{14}N transition frequency decreases by 34%. Since two-thirds of either ^{14}N means one third of the entire ^{14}N nuclei, the decrease by 34% is similar to the fraction of replacement.

(6) Decrease in the modulation depth (Case III: two non-equivalent nitrogen nuclei)

One may also consider a third system where two distinguishable ^{14}N nuclear spins and one ^{1}H nuclear spin are coupled to the same electron spin. If a fraction of either ^{14}N is replaced with ^{15}N, the signal becomes:

$$V^{p}_{14,14',15,1}(\tau, T) = p\,V_{14,15,1}(\tau, T) + (1-p)\,V_{14,14',1}(\tau, T) \quad \text{[S-53]}$$

where p is the fraction of ^{14}N replaced with ^{15}N and

$$V_{14,14',1}(\tau, T) = \frac{1}{2}\Big[V^{\alpha}_{14}(\tau, T)\,V^{\alpha}_{14'}(\tau, T)\,V^{\alpha}_{1}(\tau, T) + V^{\beta}_{14}(\tau, T)\,V^{\beta}_{14'}(\tau, T)\,V^{\beta}_{1}(\tau, T)\Big] \quad \text{[S-54]}$$

$$V_{14,15,1}(\tau, T) = \frac{1}{2}\Big[V^{\alpha}_{14}(\tau, T)\,V^{\alpha}_{15}(\tau, T)\,V^{\alpha}_{1}(\tau, T) + V^{\beta}_{14}(\tau, T)\,V^{\beta}_{15}(\tau, T)\,V^{\beta}_{1}(\tau, T)\Big] \quad \text{[S-55]}$$

Assuming that V^{α}_{15} and V^{β}_{15} are almost 1, one can rewrite eq [S-55] as:

$$V_{14,15,1}(\tau, T) = \frac{1}{2}\Big[V^{\alpha}_{14}(\tau, T)\,V^{\alpha}_{1}(\tau, T) + V^{\beta}_{14}(\tau, T)\,V^{\beta}_{1}(\tau, T)\Big] \quad \text{[S-56]}$$

Expansion of eq [S-53] gives an equation that contains the zero-frequency part and the oscillating part. The sum of the coefficients of the terms containing either S^{α}_{14} or $S^{\alpha}_{14'}$, $B^{p}_{14\text{–}15}$, is:

$$B^{p}_{14\text{–}15} = \frac{1-K_1}{2}\Big[K^{\alpha}_{14} + (1-p)K^{\alpha}_{14'} - 2(1-p)K^{\alpha}_{14}K^{\alpha}_{14'}\Big] \quad \text{[S-57]}$$

Also, the coefficient of the term containing S_1, $D^{p}_{14\text{–}15}$, is:

$$D^{p}_{14\text{–}15} = \frac{K_1}{2}\Big[(1-p)(K^{\alpha}_{14}K^{\alpha}_{14'} + K^{\beta}_{14}K^{\beta}_{14'} - K^{\alpha}_{14'} - K^{\beta}_{14'}) - (K^{\alpha}_{14} + K^{\beta}_{14}) + 2\Big] \quad \text{[S-58]}$$

The ratio of $B^{p}_{14\text{–}15}$ to $D^{p}_{14\text{–}15}$ is expressed as:

$$B^{p}_{14\text{–}15}/D^{p}_{14\text{–}15} = \frac{(1-K_1)[K^{\alpha}_{14} + (1-p)K^{\alpha}_{14'} - 2(1-p)K^{\alpha}_{14}K^{\alpha}_{14'}]}{K_1[(1-p)(K^{\alpha}_{14}K^{\alpha}_{14'} + K^{\beta}_{14}K^{\beta}_{14'} - K^{\alpha}_{14'} - K^{\beta}_{14'}) - (K^{\alpha}_{14} + K^{\beta}_{14}) + 2]} \quad \text{[S-59]}$$

As already shown in eqs [S-41] and [S-50], one can calculate the decrease in the sum of the relative modulation depths of the ^{14}N nuclear transition frequencies by comparing ${B^p}_{14\text{–}15}/{D^p}_{14\text{–}15}$ with ${B^0}_{14\text{–}15}/{D^0}_{14\text{–}15}$, that is, $B_{2'}/D_{2'}$ in eq [S-31].

$$F(p\ ^{15}\mathrm{N}/0\ ^{15}\mathrm{N}) = \frac{{B^p}_{14\text{–}15}/{D^p}_{14\text{–}15}}{B_{2'}/D_{2'}}$$
$$= \frac{[K^{\alpha}_{14} + (1-p)K^{\alpha}_{14'} - 2(1-p)K^{\alpha}_{14}K^{\alpha}_{14'}][(1-K^{\alpha}_{14})(1-K^{\alpha}_{14'}) + (1-K^{\beta}_{14})(1-K^{\beta}_{14'})]}{(K^{\alpha}_{14} + K^{\alpha}_{14'} - 2K^{\alpha}_{14}K^{\alpha}_{14'})[(1-p)(K^{\alpha}_{14}K^{\alpha}_{14'} + K^{\beta}_{14}K^{\beta}_{14'} - K^{\alpha}_{14'} - K^{\beta}_{14'}) - (K^{\alpha}_{14} + K^{\beta}_{14}) + 2]} \quad \text{[S-60]}$$

If p is 1, eq [S-60] becomes:

$$F(1\ ^{15}\mathrm{N}/0\ ^{15}\mathrm{N}) = \frac{K^{\alpha}_{14}[(1-K^{\alpha}_{14})(1-K^{\alpha}_{14'}) + (1-K^{\beta}_{14})(1-K^{\beta}_{14'})]}{(K^{\alpha}_{14} + K^{\alpha}_{14'} - 2K^{\alpha}_{14}K^{\alpha}_{14'})(2 - K^{\alpha}_{14} - K^{\beta}_{14})} \quad \text{[S-61]}$$

The right-hand side of eq [S-61] is the reciprocal of eq [S-32], which explains the increase in the sum of the relative modulation depths of the ^{14}N nuclear transition frequencies with an additional ^{14}N nucleus that is distinguishable from the other ^{14}N nucleus. On the other hand, if K^{α}_{14}, $K^{\alpha}_{14'}$, K^{β}_{14}, and $K^{\beta}_{14'}$ are much smaller than 1, the factor converges to $1 - pq/(q+1)$, where q is the ratio of $K^{\alpha}_{14'}$ to K^{α}_{14}. If the K^{α}_{14}, $K^{\alpha}_{14'}$, K^{β}_{14}, and $K^{\beta}_{14'}$ values are assumed to be 0.150, eq [S-60] becomes:

$$F(p\ ^{15}\mathrm{N}/0\ ^{15}\mathrm{N}) = \frac{1.445\,(0.255 - 0.105\,p)}{0.255\,(1.445 + 0.255\,p)} \quad \text{[S-62]}$$

In the case that two-thirds of either ^{14}N is replaced with ^{15}N, the ratio $F(p\ ^{15}\mathrm{N}/0\ ^{15}\mathrm{N})$ is approximately 0.649, which indicates that the sum of the relative modulation depths of the ^{14}N transition frequencies decreases by 35.1%. Since two-thirds of either ^{14}N means one third of the entire ^{14}N nuclei, the decrease by 35.1% is similar to the fraction of replacement, which is approximately 33.3%.

(7) Use of definite integrals instead of modulation depths

Since an ESEEM time-domain signal may contain modulations at several different frequencies, it is often difficult to obtain the modulation depths of some frequencies. The modulation at each frequency can be expressed as the product of a constant and a damped oscillating function. Also, it has already been shown that the coefficient of the damped oscillating function depends on the fraction of a certain type of nucleus replaced, f. Therefore, a general three-pulse ESEEM signal with l different frequencies is given by:

$$V(\tau,\, T,\, f) = K_0(\tau,\, f)\, S_0(T) + \sum_{i=1}^{l} K_i(\tau,\, f)\, S_i(\tau,\, T) \quad (i = 1,\, 2,\, 3,\, \cdots,\, l) \qquad \text{[S-63]}$$

where K_i $(i = 0,\, 1,\, 2,\, \cdots,\, l)$ and S_i $(i = 1,\, 2,\, 3,\, \cdots,\, l)$ are the amplitude parameter and the damped oscillating function of the modulation at *i*th frequency, ω_i, respectively, and S_0 is a decay function. The ratio of the modulation depth of the frequency ω_a to that of the frequency ω_b is K_a/K_b. Then, the Fourier transform of $V(\tau,\, T,\, f)$ with respect to T is given by:

$$\mathcal{V}(\tau,\, \omega,\, f) = K_0(\tau,\, f)\, \mathcal{S}_0(\omega) + \sum_{i=1}^{l} K_i(\tau,\, f)\, \mathcal{S}_i(\tau,\, \omega) \quad (i = 1,\, 2,\, 3,\, \cdots,\, l) \qquad \text{[S-64]}$$

where $\mathcal{S}_i$ $(i = 0,\, 1,\, 2,\, \cdots,\, l)$ is the Fourier transform of S_i. For each i $(i = 1,\, 2,\, 3,\, \cdots,\, l)$, the definite integral of the function $\mathcal{S}_i(\tau,\, \omega)$ through the spectral bandwidth in the (angular) frequency domain is considered and denoted as $\mathcal{I}_i(\tau)$.

$$\mathcal{I}_i(\tau) = \int_{-\omega_{BW}}^{\omega_{BW}} \mathcal{S}_i(\tau,\, \omega)\, dw \qquad \text{[S-65]}$$

where ω_{BW} and $-\omega_{BW}$ are the upper limit and the lower limit of the spectral bandwidth, respectively. Since the function $\mathcal{S}_i(\tau,\, \omega)$ is peaked at a specific frequency of ω_i, the integral from $\omega_i - \delta\omega_i$ to $\omega_i + \delta\omega_i$ with an appropriate $\delta\omega_i$ can account for a significant portion of the integral $\mathcal{I}_i(\tau)$. If an

absorptive Lorentzian curve with a full-width at half maximum of Γ_i is assumed, the integral $\mathcal{I}_i(\tau)$ is independent of τ and expressed as:

$$\mathcal{A}_i = \int_{-\omega_{BW}}^{\omega_{BW}} \frac{2\Gamma_i}{4(\omega-\omega_i)^2+{\Gamma_i}^2}\,d\omega = \tan^{-1}\left[\frac{2(\omega_{BW}+\omega_i)}{\Gamma_i}\right] + \tan^{-1}\left[\frac{2(\omega_{BW}-\omega_i)}{\Gamma_i}\right] \quad \text{[S-66]}$$

In eq [S-66], $\mathcal{A}_i$ is used in lieu of $\mathcal{I}_i$ to denote the absorptive Lorentzian. Similarly, the integral between $\omega_i - \delta\omega_i$ and $\omega_i + \delta\omega_i$, ${\mathcal{A}_i}^{\delta\omega_i}$, is:

$${\mathcal{A}_i}^{\delta\omega_i} = 2\tan^{-1}\left(\frac{2\delta\omega_i}{\Gamma_i}\right) \quad \text{[S-67]}$$

It is obvious that the ratio of ${\mathcal{A}_i}^{\delta\omega_i}$ to $\mathcal{A}_i$ is larger with a smaller Γ_i value. Calculations show that the ratio, ${\mathcal{A}_i}^{\delta\omega_i}/\mathcal{A}_i$, is greater than 0.8, 0.9, and 0.95 with a $\delta\omega_i$ value of 1.5, 2.9, and 5.3 MHz, respectively, provided that a Γ_i value of 1 MHz and a spectral bandwidth of 62.5 MHz are assumed. Also, it is noteworthy that the ratio ${\mathcal{A}_i}^{\delta\omega_i}/\mathcal{A}_i$ is a function of ω_i, $\delta\omega_i$, Γ_i, and ω_{BW}.

Even though the absorptive Lorentzian lineshape leads to a better resolved spectrum, a magnitude spectrum is more generally obtained due to the phase difference. If a peak with a full-width at half maximum of Γ_i in a magnitude spectrum is considered, the integral $\mathcal{I}_i(\tau)$ is given by:

$$\begin{aligned}\mathcal{M}_i &= \int_{-\omega_{BW}}^{\omega_{BW}} \frac{2\sqrt{3}}{\sqrt{12(\omega-\omega_i)^2+{\Gamma_i}^2}}\,d\omega \\ &= \ln\left[\frac{\left[\sqrt{12(\omega_{BW}+\omega_i)^2+{\Gamma_i}^2}+2\sqrt{3}(\omega_{BW}+\omega_i)\right]\left[\sqrt{12(\omega_{BW}-\omega_i)^2+{\Gamma_i}^2}+2\sqrt{3}(\omega_{BW}-\omega_i)\right]}{{\Gamma_i}^2}\right]\end{aligned} \quad \text{[S-68]}$$

In eq [S-68], $\mathcal{M}_i$ is used to denote the magnitude spectrum. Likewise, the integral between $\omega_i - \delta\omega_i$ and $\omega_i + \delta\omega_i$, ${\mathcal{M}_i}^{\delta\omega_i}$, is:

$${\mathcal{M}_i}^{\delta\omega_i} = 2\ln\left(\frac{\sqrt{12{\delta\omega_i}^2+{\Gamma_i}^2}+2\sqrt{3}\,\delta\omega_i}{\Gamma_i}\right) \quad \text{[S-69]}$$

Like $\mathcal{A}_i^{\delta\omega_i}/\mathcal{A}_i$, the ratio of $\mathcal{M}_i^{\delta\omega_i}$ to $\mathcal{M}_i$ is larger with a smaller Γ_i value and a function of ω_i, $\delta\omega_i$, Γ_i, and ω_{BW}. Calculations show that the ratio, $\mathcal{M}_i^{\delta\omega_i}/\mathcal{M}_i$, is greater than 0.5, 0.6, 0.7, and 0.8 with a $\delta\omega_i$ value of 2.1 3.6, 6.2, and 10.7 MHz, respectively, provided that a Γ_i value of 1 MHz and a spectral bandwidth of 62.5 MHz are assumed.

In eq [S-63], the relative modulation depth of the frequency ω_a, which is defined as the modulation depth of the frequency ω_a normalized by the that of the frequency ω_b, is denoted as $K_a(\tau,\, f)/K_b(\tau,\, f)$. According to eqs [S-64] and [S-65], the integrals of the frequencies ω_a and ω_b in the (angular) frequency domain are expressed as $K_a(\tau,\, f)\,\mathcal{I}_a(\tau)$ and $K_b(\tau,\, f)\,\mathcal{I}_b(\tau)$, respectively. Since magnitude spectra are obtained in our experiments, the integrals can be rewritten as $K_a(\tau,\, f)\,\mathcal{M}_a$ and $K_b(\tau,\, f)\,\mathcal{M}_b$, respectively. Then, the relative integral of the frequency ω_a, which is defined as the integral of the frequency ω_a normalized by the integral of the frequency ω_b, is $K_a(\tau,\, f)\,\mathcal{M}_a/K_b(\tau,\, f)\,\mathcal{M}_b$.

If no ^{14}N nucleus is replaced with ^{15}N, the fraction of ^{15}N, f, is 0. The relative modulation depth of the frequency ω_a in the time domain becomes $K_a(\tau,\, 0)/K_b(\tau,\, 0)$ and its relative integral in the (angular) frequency domain becomes $K_a(\tau,\, 0)\,\mathcal{M}_a/K_b(\tau,\, 0)\,\mathcal{M}_b$. As already shown in eqs [S-41] and [S-50], one can calculate the decrease in the relative modulation depth of the frequency ω_a by comparing $K_a(\tau,\, f)/K_b(\tau,\, f)$ with $K_a(\tau,\, 0)/K_b(\tau,\, 0)$.

$$F_K(f\ ^{15}\mathrm{N}/0\ ^{15}\mathrm{N}) = \frac{K_a(\tau,\, f)/K_b(\tau,\, f)}{K_a(\tau,\, 0)/K_b(\tau,\, 0)} \qquad \text{[S-70]}$$

where the subscript K denotes the comparison of modulation depths. Similarly, the decrease in the relative integral of the frequency is calculated by comparing $K_a(\tau,\, f)\,\mathcal{M}_a/K_b(\tau,\, f)\,\mathcal{M}_b$ with $K_a(\tau,\, 0)\,\mathcal{M}_a/K_b(\tau,\, 0)\,\mathcal{M}_b$.

$$F_I(f\ ^{15}\mathrm{N}/0\ ^{15}\mathrm{N}) = \frac{K_a(\tau,\, f)\,\mathcal{M}_a/K_b(\tau,\, f)\,\mathcal{M}_b}{K_a(\tau,\, 0)\,\mathcal{M}_a/K_b(\tau,\, 0)\,\mathcal{M}_b} = \frac{K_a(\tau,\, f)/K_b(\tau,\, f)}{K_a(\tau,\, 0)/K_b(\tau,\, 0)} \qquad \text{[S-71]}$$

where the subscript I denotes the comparison of integrals. It is concluded from eq [S-71] that the decrease in the relative integral is the same as that in the modulation depth. Also, if the integral between

$\omega_a - \delta\omega_a$ and $\omega_a + \delta\omega_a$, $\mathcal{M}_a^{\delta\omega_a}$, and the integral between $\omega_b - \delta\omega_b$ and $\omega_b + \delta\omega_b$, $\mathcal{M}_b^{\delta\omega_b}$, are used instead of $\mathcal{M}_a$ and $\mathcal{M}_b$, respectively, the decrease in the new relative integral of the frequency is expressed as:

$$F_I^{\delta}(f\ ^{15}\mathrm{N}/0\ ^{15}\mathrm{N}) = \frac{K_a(\tau,\, f)\,\mathcal{M}_a^{\delta\omega_a}/K_b(\tau,\, f)\,\mathcal{M}_b^{\delta\omega_b}}{K_a(\tau,\, 0)\,\mathcal{M}_a^{\delta\omega_a}/K_b(\tau,\, 0)\,\mathcal{M}_b^{\delta\omega_b}} = \frac{K_a(\tau,\, f)/K_b(\tau,\, f)}{K_a(\tau,\, 0)/K_b(\tau,\, 0)} \qquad \text{[S-72]}$$

where the superscript δ denotes the integral over a part of the spectral bandwidth. Therefore, the comparison of the integrals over a part of the spectral bandwidth can be used for the same purpose.

In fact, the relatively broad lineshape of magnitude spectra might cause significant overlaps of two or more peaks in some frequency regions. In addition, magnitude spectra essentially have cross-term errors. A large difference in frequencies may alleviate these problems. We use the ^{14}N transition frequencies ranging approximately from 0.5 MHz to 5 MHz and the transition frequency of a weakly coupled ^{1}H nuclear spin, whose Larmor frequency ranges between 11 MHz and 15.5 MHz with a magnetic field swept from 2600 G to 3600 G. Calculations reveal that when the difference in two frequencies and the full-width at half maximum are assumed to be 10 MHz and 1 MHz, respectively, the intensity of one magnitude Lorentizan line at the peak of the other magnitude Lorentzian line is less than 2.9% the intensity at its own peak.

(8) Calculation of the definite integrals of some simulated three-pulse ESEEM spectra

Figure S10 illustrates the simulated three-pulse ESEEM spectra of two systems with different numbers of coupled ^{14}N nuclear spins. One ^{14}N nuclear spin and one weakly coupled ^{1}H nuclear spin are assumed for the spectrum in gray whereas two equivalent ^{14}N nuclei and one weakly coupled ^{1}H nucleus are for the spectrum in black. The ^{14}N-ESEEM parameters used for both spectra are identical to those for Component I in **Table S7** and the frequency and modulation depth of the ^{1}H-ESEEM are 14.3 MHz and 0.05, respectively.

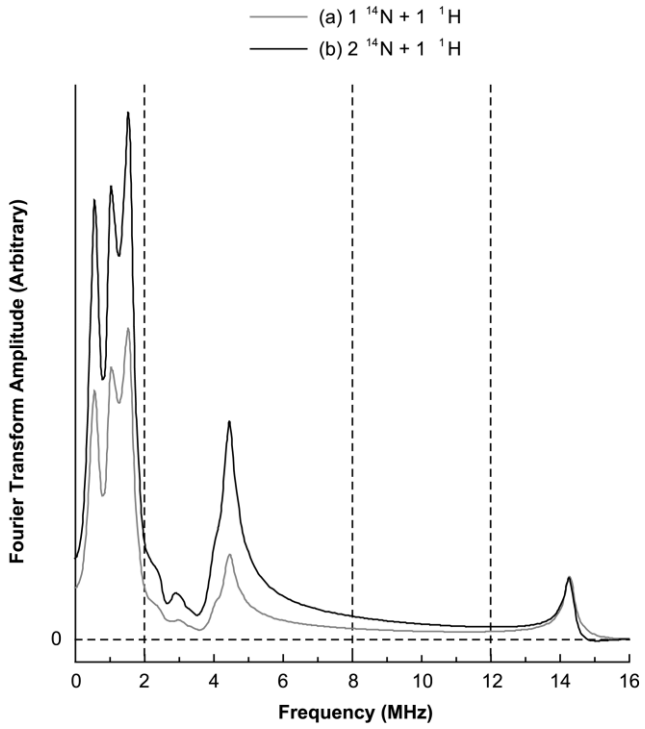

Figure S10. Simulated three-pulse ESEEM spectra of an electron spin system to which one ^{14}N and one ^{1}H nuclear spin are coupled and another electron spin system to which two equivalent ^{14}N nuclear spins and one ^{1}H nuclear spin are coupled. The vertical dashed lines separate the NQI region (0–2 MHz), DQ region (2–8 MHz), and ^{1}H-ESEEM region (12–16 MHz).

When the nuclear quadrupole interaction (NQI) region and DQ region of the ^{14}N-ESEEM are considered together, the normalized ^{14}N-ESEEM intensity of the system with two ^{14}N nuclear spins is approximately 1.78 times as much as that of the system with only one ^{14}N as shown in **Table S8**. The approximately 11% deviation from 2 may be explained by the modulation depths that are not small enough to ignore. However, when the NQI region of the ^{14}N-ESEEM, which is between 0 and 2 MHz, or the DQ region, which is roughly between 2 and 8 MHz, is considered separately, the ratio between the two normalized ^{14}N-ESEEM intensities changes. In eq [S-24], the ratio $F(2\ ^{14}\mathrm{N}/1\ ^{14}\mathrm{N})$ depends on the modulation depths of the frequencies in both electron spin manifolds. Also, it is expected from the equation that the ratio $F(2\ ^{14}\mathrm{N}/1\ ^{14}\mathrm{N})$ is smaller for the electron spin manifold with the deeper modulation than the other electron spin manifold. For weakly coupled ^{14}N nuclear spins, the frequencies in the α manifold have deeper modulations than those in the β manifold as the former and the latter

correspond to the NQI transition and the DQ transition, respectively. In our simulations, the ratios for the NQI region and the DQ region are 1.57 and 2.23, respectively, which is consistent with the expectation. The negative deviation from 2 is possibly due to the deeper modulations of the frequencies in the α manifold while the positive deviation from 2 may be accounted for by some combinations or harmonics of the fundamental NQI transition frequencies.

Table S8. Relative integrated intensities of the simulated ESEEM spectra of two systems with different numbers of coupled ^{14}N nuclear spins. The integrated intensities of the ^{14}N-ESEEM region (0–8 MHz), which includes the NQI region (0–2 MHz) and the DQ region (2–8 MHz), are normalized by those of the ^{1}H-ESEEM region (12–16 MHz).

	(a) ^{14}N-ESEEM	(b) ^{1}H-ESEEM	[(a) / (b)][a]	$F_I^{\delta}(2\,\mathrm{N}/1\,\mathrm{N})$[b]
^{14}N-ESEEM region (0–8 MHz) and ^{1}H-ESEEM region (12–16 MHz)				
1 ^{14}N + 1 ^{1}H	1340	141	9.50	1.78
2 ^{14}N + 1 ^{1}H	2590	154	16.9	
NQI ^{14}N-ESEEM region (0–2 MHz) and ^{1}H-ESEEM region (12–16 MHz)				
1 ^{14}N + 1 ^{1}H	944	141	6.70	1.57
2 ^{14}N + 1 ^{1}H	1620	154	10.5	
DQ ^{14}N-ESEEM region (2–8 MHz) and ^{1}H-ESEEM region (12–16 MHz)				
1 ^{14}N + 1 ^{1}H	399	141	2.83	2.23
2 ^{14}N + 1 ^{1}H	971	154	6.32	

[a] Normalized ^{14}N-ESEEM intensity.

[b] Ratio of the normalized ^{14}N-ESEEM intensities between the two systems.

To assess the contribution of each histidine residue to the Cu(II) coordination in the Cu(II)–Aβ(1–16) and dien–Cu(II)–Aβ(1–16) complexes, we compare the decrease in the normalized ^{14}N-ESEEM intensity caused by replacing ^{14}N of either His6, His13, or His14 with ^{15}N. It is assumed that the ESEEM-active ^{14}N nuclei of all the three residues have almost identical ESEEM parameters including e^2qQ/h, η, A_{iso}, and $|T|$ because there is little difference in the spectral shape between the nonlabeled

versions and their ^{15}N-labeled counterparts irrespective of which residue is ^{15}N-enriched. Thus, one can consider the ESEEM-active ^{14}N nuclei of the three residues to be equivalent, which means that the frequencies and their modulation depths attributed to the three residues are essentially identical to one another.

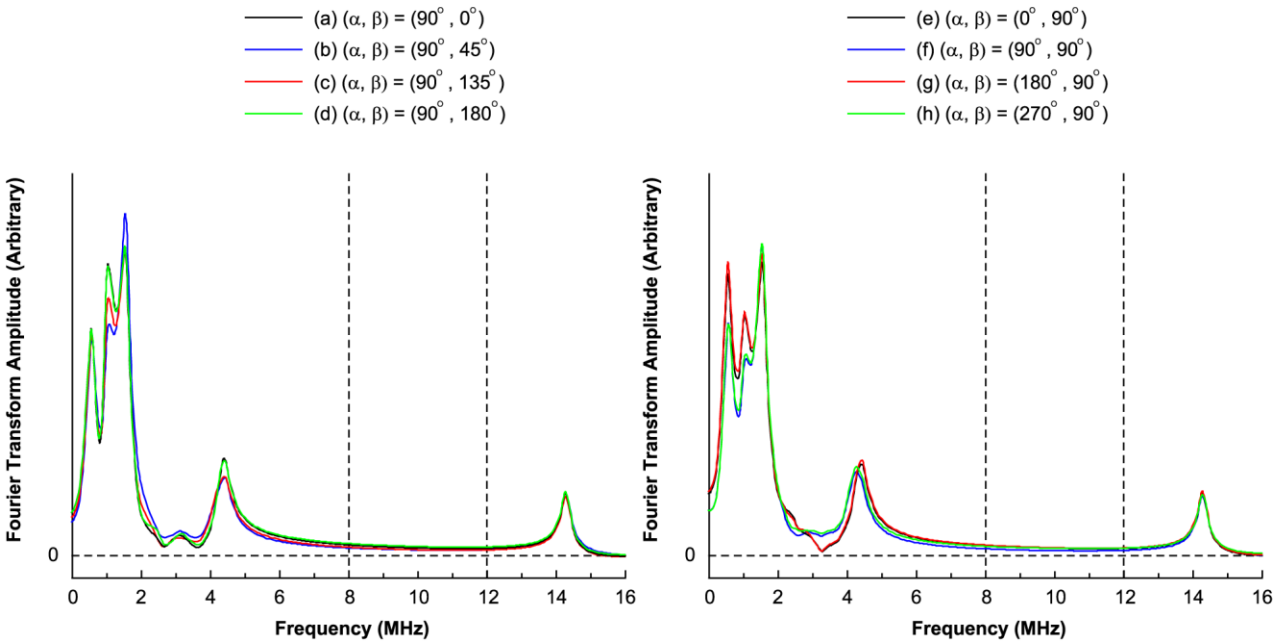

Figure S11. Simulated three-pulse ESEEM spectra of an electron spin system to which one ^{14}N and one ^{1}H nuclear spin are coupled with different Euler angles. The vertical dashed lines separate the ^{14}N-ESEEM region (0–8 MHz) and ^{1}H-ESEEM region (12–16 MHz).

Our simulations reveal that the spectral shape of the three-pulse ESEEM spectrum may depend on the Euler angles between the quadrupole tensor and the hyperfine tensor when the other NQI and hyperfine parameters are identical. In the Cu(II)–Aβ(1–16) complex, the Euler angles of the ESEEM-active ^{14}N nuclei of two different histidine residues might be different because the two residues simultaneously coordinate to Cu(II). Nevertheless, only little difference in the angles or little dependency of the spectral shape on the angles is expected between the two simultaneously Cu(II)-coordinated histidine residues because different angles may lead to noticeably different spectral shapes. **Figure S11** shows the difference in spectral shape due to different Euler angles. Again, the NQI and hyperfine parameters, other than the angles, used for the simulated spectra are identical to those for Component I in **Table S7**

and the frequency and modulation depth of the ^{1}H-ESEEM are 14.3 MHz and 0.05, respectively. While the three NQI frequencies remain identical, the double-quantum frequency is affected by the angles. Interestingly, the normalized ^{14}N-ESEEM intensity varies only within 5% of the average value in spite of the different spectral shapes due to the different Euler angles. Therefore, if the difference in the normalized ^{14}N-ESEEM intensity between two of the three ^{15}N-labeled Cu(II)–Aβ(1–16) complexes is larger than the expected deviation, it is probable that the difference results, at least partially, from the different contributions of the two histidine residues. The relative intensities of the simulated ESEEM spectra are displayed in **Table S9**.

Table S9. Relative integrated intensities of the simulated ESEEM spectra of an electron spin system to which one ^{14}N spin is coupled with different Euler angles. The integrated intensities of the ^{14}N-ESEEM region (0–8 MHz), which includes the NQI region (0–2 MHz) and the DQ region (2–8 MHz), are normalized by those of the ^{1}H-ESEEM region (12–16 MHz).

α, β (°)	(a) ^{14}N-ESEEM	(b) ^{1}H-ESEEM	[(a) / (b)][a]	deviation[b] (%)
90, 0	1320	142	9.30	-0.07 (-0.8%)
90, 15	1210	132	9.17	-0.20 (-2.2%)
90, 30	1180	132	8.94	-0.43 (-4.6%)
90, 45	1190	131	9.08	-0.29 (-3.1%)
90, 60	1220	135	9.04	-0.33 (-3.5%)
90, 75	1280	141	9.08	-0.29 (-3.1%)
90, 90	1270	136	9.34	-0.03 (-0.3%)
90, 105	1310	137	9.56	0.19 (2.0%)
90, 120	1280	136	9.41	0.04 (0.4%)
90, 135	1290	137	9.42	0.05 (0.5%)
90, 150	1280	136	9.42	0.05 (0.5%)
90, 165	1230	131	9.39	0.02 (0.2%)
90, 180	1320	142	9.30	-0.07 (-0.8%)
0, 90	1460	149	9.80	0.43 (4.6%)
45, 90	1340	141	9.50	0.13 (1.4%)
135, 90	1370	141	9.72	0.35 (3.7%)

180, 90	1450	148	9.80	0.43 (4.6%)
225, 90	1360	145	9.38	0.01 (0.1%)
270, 90	1290	136	9.49	0.12 (1.3%)
315, 90	1360	143	9.51	0.14 (1.5%)
0, 45	1370	147	9.32	-0.05 (-0.5%)
180, 45	1330	141	9.43	0.06 (0.6%)
270, 45	1310	135	9.70	0.33 (3.5%)
0, 135	1350	146	9.25	-0.12 (-1.3%)
180, 135	1320	141	9.36	-0.01 (-0.1%)
270, 135	1200	134	8.96	-0.41 (-4.4%)
average			9.37	0

[a] Normalized ^{14}N-ESEEM intensity.

[b] Deviation and the ratio of the deviation to the average in the parentheses.

References

(1) McCracken, J.; Pember, S.; Benkovic, S. J.; Villafranca, J. J.; Miller, R. J.; Peisach, J. *J. Am. Chem. Soc.* **1988**, *110*, 1069–1074.

(2) Lee, H.-I.; Doan, P. E.; Hoffman, B. M. *J. Magn. Reson.* **1999**, *140*, 91–107.

(3) Stoll, S.; Britt, R. D. *Phys. Chem. Chem. Phys.* **2009**, *11*, 6614–6625.

(4) Mims, W. B. *Phys. Rev. B* **1972**, *5*, 2409–2419.

(5) Dikanov, S. A.; Shubin, A. A.; Parmon, V. N. *J. Magn. Reson.* **1981**, *42*, 474–487.

(6) Stoll, S.; Calle, C.; Mitrikas, G.; Schweiger, A. *J. Magn. Reson.* **2005**, *177*, 93–101.